



ELSEVIER

Contents lists available at ScienceDirect

Earth-Science Reviews

journal homepage: www.elsevier.com/locate/earscirev

Quantitative analysis of the stratigraphic architecture of incised-valley fills: A global comparison of Quaternary systems



Ru Wang*, Luca Colombera, Nigel P. Mountney

Fluvial & Eolian Research Group and Shallow-Marine Research Group, School of Earth & Environment, University of Leeds, Leeds, LS2 9JT, UK

ARTICLE INFO

Keywords:

Incised valley
Sea-level change
Continental margin
Quaternary
Drainage basin
Hydrodynamics

ABSTRACT

Facies models of the internal fills of incised valleys developed in shelf and coastal settings during cycles of relative sea-level change are largely conceptual, descriptive and qualitative in form; moreover, they are commonly bespoke to individual examples. Here, a database-driven quantitative statistical analysis of 87 late-Quaternary incised-valley fills (IVFs) has been undertaken to assess the general validity and predictive value of classical facies models for IVFs, and to investigate the relative importance of possible controls on their stratigraphic organization. Based on datasets from the published literature stored in a sedimentological database, the geometry and proportion of systems tracts, and of architectural elements of different hierarchies within IVFs are quantified. These variables were analysed to assess how they vary in relation to parameters that represent potential controlling factors: relative sea-level stage, continental-margin type, drainage-basin area, valley geometry, basin physiography and shoreline hydrodynamics.

The stratigraphic organization of the studied coastal-plain IVFs is generally consistent with that represented in facies models, the primary control being the rate and magnitude of relative sea-level change. However, results from this study demonstrate significant variability in the stratigraphic architectures of IVFs, which is not accounted for by existing models. Variations in the facies architecture of coastal-plain and cross-shelf valley fills can be attributed to controls other than sea level, and expressed in relationships with continental-margin type, basin physiography, catchment area, river-system size and shoreline hydrodynamics. The following primary findings arise from this research. (i) Compared to their counterparts on passive margins, coastal-plain IVFs hosted on active margins contain, on average, a higher proportion of fluvial deposits and a lower proportion of central-basin estuarine deposits; estuarine deposits tend however to be thicker. This suggests a control on IVF stratigraphic architecture exerted by distinct characteristics of the tectonic setting of the host continental margins, notably basin physiography, rates and mode of sediment supply, and nature of sediment load. (ii) The thickness and proportion of lowstand systems tract are positively correlated with coastal-plain IVF dimensions, likely reflecting the role of drainage-basin area in dictating the scale of the fluvial systems that carved and infilled the valleys. (iii) Positive correlations are observed between the thickness of fluvial deposits, bayhead-delta deposits and central-basin estuarine deposits, versus coastal-plain IVF dimensions and valley catchment area. This suggests a control exerted by the river-system scale on sediment-supply rates and on the accommodation determined by valley size. (iv) Positive correlations between the thickness and proportion of barrier-complex deposits within cross-shelf IVFs versus mean shelf gradient indicate that the geometry of the shelf might control the establishment and preservation of barrier-island environments in incised valleys located on the shelf. (v) Correlations between the width of coastal-plain IVFs and present-day mean tidal range at the shoreline indicate that tidal dynamics may contribute to the widening of the incised valleys. Positive correlation is observed between the proportion of tide-dominated elements in highstand IVF deposits and IVF width, suggesting possible effects of interplays between hydrodynamic conditions and the geometry of incised valleys on their infills.

This study highlights the complexity of the internal fills of incised valleys, which must be considered when attempting the application of facies models of IVFs to rock-record interpretations or as predictive tools in subsurface studies.

* Corresponding author.

E-mail address: eerw@leeds.ac.uk (R. Wang).<https://doi.org/10.1016/j.earscirev.2019.102988>

Received 3 June 2019; Received in revised form 28 August 2019; Accepted 21 October 2019

Available online 06 November 2019

0012-8252/ © 2019 The Authors. Published by Elsevier B.V. This is an open access article under the CC BY license

[\(http://creativecommons.org/licenses/by/4.0/\)](http://creativecommons.org/licenses/by/4.0/).

1. Introduction

Incised valleys are fluvially eroded, elongate palaeotopographic lows developed in shelf and coastal settings during episodes of relative sea-level fall, and subsequently inundated, infilled and reworked by fluvial, coastal and marine processes during sea-level rise (Posamentier and Allen, 1999; Dalrymple and Zaitlin, 1994; Blum et al., 2013). The fills of incised valleys represent critical stratigraphic archives of environmental change in coastal regions, in response to changes in sea level and climate. They are especially important in this regard as adjacent shelf areas commonly store a less complete sedimentary record because of physical reworking and/or sediment starvation (Boyd et al., 2006; Simms et al., 2010; Mattheus and Rodriguez, 2011). For this reason, the fills of incised valleys have also been the subject of detailed sequence stratigraphic analyses (e.g., Lin et al., 2005; Dalrymple, 2006; Chaumillon et al., 2010). Additionally, valley infills are important hydrocarbon reservoir targets and they also serve as reference for exploration of downdip deep-marine sands (Dalrymple et al., 1994; Shanley and McCabe, 1994; Dalrymple and Zaitlin, 1994; Blum et al., 2013). Therefore, predictions of the internal sedimentary architecture of valley infills are desirable in subsurface characterization and hydrocarbon exploration workflows (e.g., Hampson et al., 1999; Stephen and Dalrymple, 2002; Bowen and Weimer, 2003; Salem et al., 2005). Furthermore, in many present-day settings, estuaries and rias that commonly develop at the mouths of incised valleys during sea-level rise, accommodate large and dense human populations and constitute fragile coastal settings of primary economic and ecological importance (Kennish, 1991; Chaumillon et al., 2010; Zhang et al., 2014; Marlianingrum et al., 2019).

Given the scientific, economic and ecological importance of incised-valley fills (IVFs), extensive research has been undertaken to characterise their stratigraphic organization (e.g., Roy, 1984; Dalrymple et al., 1992; Allen and Posamentier, 1993, 1994b; Dalrymple and Zaitlin, 1994; Boyd et al., 2006; Blum et al., 2013). Widely adopted models of coastal-plain incised-valley development and infill (Dalrymple et al., 1992; Allen and Posamentier, 1994b; Dalrymple and Zaitlin, 1994) typically envisage three segments: (i) a proximal landward segment mostly occupied by fluvial systems throughout its depositional history; (ii) a medial segment recording a drowned-valley estuarine complex that existed around the time of maximum transgression, overlying a lowstand to transgressive succession of fluvial and estuarine deposits; and (iii) a seaward segment typically comprising basal fluvial deposits overlain by estuarine deposits and capped by fully marine deposits. Considerable prior research has focussed on the analysis of individual case-study examples whereby comparisons are made between the internal fills of individual incised valleys and the general stratigraphic organization of incised-valley fills depicted by the above-mentioned “classical” models. Individual examples have been considered in detail to document and decipher the relative importance of distinct controlling factors responsible for sedimentological complexity, notably sea level, tectonics, sediment supply, antecedent topography and hydrodynamics. As such, the great majority of current models with which to account for the internal fills of incised valleys are either bespoke to individual case-study examples, else are largely conceptual, descriptive and qualitative in form.

In this study, a database-driven approach has been taken, the aim being to quantitatively document and account for the wide variability in facies architecture present across a large number of globally distributed incised-valley fills. This approach seeks to assess the general validity of classical facies models that remain widely employed as predictive tools, and to investigate the relative importance of possible controls on the stratigraphic organization of incised-valley fills quantitatively. This work is based on a synthesis of 87 late-Quaternary incised-valley fills from the published literature, the majority of which formed during the last glacio-eustatic cycle. The incised-valley fills considered in this work only comprise of valley systems carved in

response to relative sea-level falls and infilled by alluvial, transitional (i.e., paralic) and shallow-marine strata in shelf and coastal-plain settings (Van Wagoner et al., 1990; Boyd et al., 2006; Blum et al., 2013); inland alluvial valleys are not considered. The studied examples are representative of different climatic, hydrodynamic and tectonic settings, and are distributed globally. By restricting the scope of investigation to late-Quaternary examples, the principal controlling factors that govern valley-fill characteristics – such as the rate and magnitude of sea-level change, sediment supply, antecedent topography, hydrodynamics and tectonics – can be constrained closely. This is made possible by the widespread availability of large amounts of published data (e.g., shallow seismic, core logs, dating methods) describing the late-Quaternary stratigraphic record.

Specific objectives of this work are as follows: (i) to undertake a comprehensive quantitative analysis of the geometry, spatial relationships, stacking patterns, and lithological heterogeneity of deposits that form the infill of late-Quaternary incised valleys documented in the published literature; (ii) to illustrate the variability in sedimentary architectures seen in the studied incised-valley fills with respect to facies models; (iii) to evaluate the relative roles of possible controls in determining the internal fills of incised valleys; and (iv) to present implications of the results for sequence-stratigraphic models and for subsurface-reservoir prediction and characterization.

2. Methodology

A database approach based on the synthesis of data from 87 late-Quaternary incised-valley fills is utilized. Data on the sedimentology of these incised-valley fills are included in a relational database, the Shallow-Marine Architecture Knowledge Store (SMAKS; Colombera et al., 2016). SMAKS stores data on the sedimentary architecture and geomorphic organization of shallow-marine and paralic siliciclastic depositional systems; it includes quantitative and qualitative data on geological entities of different types (e.g., facies, architectural elements), and on their associated depositional systems, themselves classified on multiple parameters (e.g., shelf width, delta catchment area) and metadata (e.g., data types, data sources).

Of the 87 late-Quaternary incised-valley fills considered in this study, 85 developed during the last glacial–interglacial cycle (LGC); two are of pre-LGC age. The primary data have been derived from 77 published literature sources. A detailed account of the case studies included in this work, their associated bibliographic references and the types of data used in each is reported in Table 1; the location of the studied incised-valley fills is shown in Fig. 1. Here, an individual case study refers to either a group of genetically related incised-valley fills (occurring on the same continental shelf or coastal plain) or to a single incised-valley fill. This work does not cover all incised-valley fills documented in the scientific literature. The chosen IVFs were selected based on the availability of data that were suited to the scopes of this study. Importantly, only valley fills that represent single cycles of incision and fill are included in the database; compound valley fills that represent multiple episodes of incisions and fills, associated with different eustatic cycles were excluded (cf. Korus et al., 2008). IVFs from present-day high-latitude regions, which are likely to have recorded periglacial and paraglacial processes, were also not included. Yet, the database was compiled trying to avoid geographical bias and attempting to make the comparative study as global and wide-reaching as possible. For the studied examples, investigations of the internal fills of valleys developed in coastal-plain settings are generally based on several 1D cores and/or 1D well logs. By contrast, studies based on cross-shelf valley fills tend to be based on 2D or 3D high-resolution seismic data, in some cases calibrated by cores.

The relative importance of different controls on the internal fills of incised valleys has been interpreted from (i) comparison of descriptive statistics and associated statistical tests, and (ii) determination of correlation between variables. In this work, the database output comprises

Table 1
Case studies on late-Quaternary incised-valley fills stored in the Shallow-Marine Architecture Knowledge Store (SMAKS) database. For each case study, the table reports published literature sources, data types, and the age of formation as being either of last glacial-interglacial cycle (LGC) or pre-LGC. Case-study identification numbers (ID) relate to those coded in the SMAKS database (Colombera et al., 2016) and are referred to in following figures. N = number of incised-valley-fill elements developed for each case study, distinguished as LGC or pre-LGC.

ID	Case study	Data source	Data types	N	Age
31	Composite database, Gulf of Mexico and Atlantic Ocean, USA	Mattheus et al. (2007); Rodriguez et al. (2008); Mattheus and Rodriguez (2011), 2014	Airborne images, Shallow seismics, Well cuttings, Cores	3	LGC
38	Pilong Formation, South China Sea, Sunda Shelf	Alqahiani et al. (2015)	Cores, 3D seismics, Shallow seismics	1	LGC
39	Late Quaternary of Manfredonia Gulf, Adriatic Sea	Maselli and Trincardi (2013); Maselli et al. (2014)	Cores, Shallow seismics	1	LGC
48	New Jersey shelf, Atlantic Ocean	Nordford et al. (2005), 2006	Cores, Shallow seismics	2	LGC
49	Hervey Bay, Queensland, Australia	Payenberg et al. (2006)	Shallow seismics, Bathymetric profile	1	LGC
59	Bay of Biscay, France	Weber et al. (2004); Chaumillon and Weber (2006); Chaumillon et al. (2008)	Cores, Shallow seismics	3	LGC
60	Bay of Biscay, France	Chaumillon et al. (2008); Proust et al. (2010)	Cores, Shallow seismics	1	Pre-LGC
61	Bay of Biscay, France	Chaumillon and Weber (2006); Chaumillon et al. (2008)	Cores, Shallow seismics	1	LGC
62	Bay of Biscay, France	Proust et al. (2001); Menier (2004); Menier et al. (2006); Chaumillon et al. (2008); Menier et al. (2010)	Cores, Shallow seismics	3	LGC
67	Pleistocene of Pattani Basin, South China Sea, Gulf of Thailand	Reijnen et al. (2011)	Well cuttings, 3D seismics, Shallow seismics	2	LGC
69	Pleistocene of southern Java Sea	Posamentier (2001)	Cores, 3D seismics, Shallow seismics	1	LGC
70	Gironde incised valley, France	Allen and Posamentier (1993); Allen and Posamentier (1994a, 1994b); Lericolais et al. (2001); Fénès et al. (2010)	Cores	1	LGC
72	Late Quaternary of Tuscany, Italy	Amorosi et al. (2008), 2013; Rossi et al. (2017)	Cores	3	LGC
73	Ombone incised valley, Italy	Bellotti et al. (2004); Breda et al. (2016)	Cores	1	Pre-LGC
74	Volturno incised valley, Italy	Amorosi et al. (2012)	Cores	1	LGC
75	Biferno incised valleys, Italy	Amorosi et al. (2016)	Cores	1	LGC
76	Tiber Delta, Italy	Milli et al. (2013), 2016	Cores	1	LGC
77	Metaponto coastal plain, Italy	Cilumbriello et al. (2010); Grippa et al. (2011); Tropeano et al. (2013)	Cores, Shallow seismics	2	LGC
81	KwaZulu-Natal shelf, South Africa	Green (2009); Benallack et al. (2016)	Cores, Shallow seismics	1	LGC
83	East China Sea, China	Zhang and Li (1996); Li and Wang (1998); Li et al. (2002); Wellner and Barrek (2003); Lin et al. (2005); Li et al. (2006); Zhang et al. (2014), 2017	Cores	4	LGC
85	Kanto Plain incised valleys, Japan	Ishihara et al. (2012); Tanabe et al. (2015); Ishihara and Sugai (2017)	Cores	3	LGC
92	KwaZulu-Natal shelf, South Africa	Green and Garlick (2011); Green et al. (2013a), b	Shallow seismics	3	LGC
93	Maputo Bay, Mozambique	Green et al. (2015)	Cores, Shallow seismics	3	LGC
125	Pakarae incised valley, New Zealand	Wilson et al. (2007)	Outcrop, Cores	1	LGC
126	Isumi incised valley, Japan	Sakai et al. (2006)	Outcrop, Cores	1	LGC
127	Bay of Biscay, France	Fénès and Lericolais (2005); Chaumillon et al. (2008); Allard et al. (2009); Fénès et al. (2010)	Cores, Shallow seismics	1	LGC
132	Manawatu incised valley, New Zealand	Clement et al. (2017); Clement and Fuller (2018)	Cores, Wireline logs	1	LGC
134	Weiti incised valley, New Zealand	Heap and Nichol (1997)	Cores	1	LGC
135	Burrill Lake incised valley, New South Wales, Australia	Sloss et al. (2006)	Cores, Shallow seismics	2	LGC
136	Lake Illawarra incised valley, New South Wales, Australia	Sloss et al. (2005)	Cores, Shallow seismics	5	LGC
137	Lake Conjolia incised valley, New South Wales, Australia	Sloss et al. (2010)	Cores	4	LGC
138	North Carolina coastal-plain incised valleys, North Carolina, USA	Mattheus and Rodriguez (2014)	Cores, Shallow seismics	2	LGC
139	Lavaca incised valley, Texas, USA	Wilkinson and Byrne (1977)	Cores	1	LGC
140	Calcasieu incised valley, Louisiana, USA	Nichol et al. (1996)	Well cuttings, Shallow seismics	1	LGC
141	Late Quaternary of Gulf of Mexico, USA	Greene et al. (2007)	Cores, Shallow seismics	13	LGC
142	Nueces incised valley, Texas, USA	Simms (2005); Simms et al. (2006)	Cores, Shallow seismics	1	LGC
143	Sabine-Neches incised-valley system, USA	Anderson et al. (1991)	Cores, Shallow seismics	1	LGC
144	Trinity-San Jacinto incised-valley system, Texas, USA	Smyth (1991); Rodriguez et al. (2005)	Cores, Shallow seismics	2	LGC
146	Baffin Bay incised valley, Texas, USA	Simms et al. (2010)	Cores, Shallow seismics	2	LGC
147	Kushiro Plain incised valley, Japan	Takashimizu et al. (2016)	Cores	1	LGC
148	Echigo Plain, Japan	Tanabe et al. (2013)	Cores	1	LGC
149	Song Hong delta system, Vietnam	Tanabe et al. (2006)	Cores	1	LGC
158	Song Hong (Red River) incised valley, Gulf of Tonkin, Vietnam	Wetzel et al. (2017)	Cores, Shallow seismics, Bathymetric profile	1	LGC

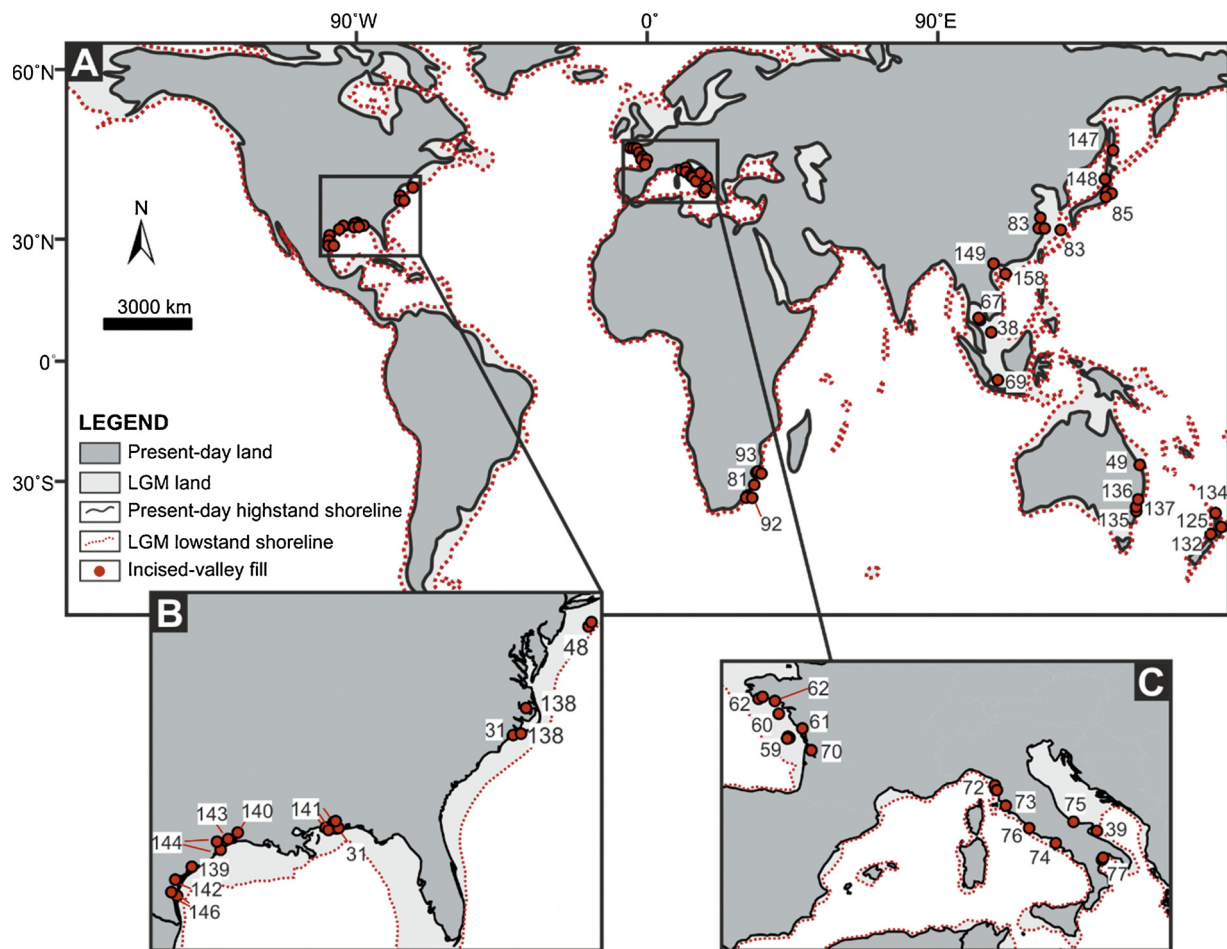


Fig. 1. (A) Geographic location of late-Quaternary incised-valley fills considered in this work, with inset maps for North America (B), and southern Europe (C). The numbers on the map correspond to the IDs in Table 1. Base map modified from Ray and Adams (2001).

the following: (i) estimations of the absolute proportion of systems tracts within incised-valley fills, computed as systems tract-to-valley-fill thickness ratio; (ii) the relative proportion of architectural elements preserved in different systems tracts within valley fills; (iii) the relative proportion of architectural elements within valley fills; and (iv) the geometry of these sedimentary bodies.

2.1. Scope of investigation

Large variations in IVF architecture and geometry exist along the dip profile of incised-valley systems (Dalrymple et al., 1992; Dalrymple and Zaitlin, 1994; Chaumillon et al., 2010; Blum et al., 2013; Strong and Paola, 2008; Martin et al., 2011; Phillips, 2011). Thus, to enable meaningful comparisons, measurements should ideally be made at the same respective location along the valley axis. However, the use of data from the published literature imposes some limitations to our ability to refer observations from different IVFs to a common reference system. In this work, observations are broadly categorized based on the position where the measurements were made, by classifying the studied valley fills depending on whether they now occur beneath present-day coastal plains or on continental shelves ($N = 61$ and 27 , respectively). For incised-valley fills that sit beneath modern coastal plains, the analyses have focussed on relationships between the proportion and geometry of architectural elements that compose them versus continental-margin type, catchment and river-system size, basin physiography and descriptors of present-day hydrodynamics. For cross-shelf valleys, relationships between shelf gradient versus the proportion and geometry of certain architectural-element types are specifically investigated in

detail.

In the analysis of properties relating to systems tracts and elements in incised-valley fills, only lowstand (LST), transgressive (TST) and highstand (HST) systems tracts are considered; falling-stage systems tracts (FSST) are discarded for this purpose, even where they are reported as part of the incised-valley fill ($N = 3$). This was done to conform to sequence stratigraphic models (cf. Helland-Hansen and Martinsen, 1996) that place the sequence boundary at the base of the LST. However, there are several cases where the deposits contained in the infill of the IVFs have not been assigned to systems tract, and it is possible that some of those deposits actually record deposition during falling stage; if these deposits were reported as contained in the IVF, they are considered in this study.

2.2. Architectural-element classifications

In the SMAKS database, architectural elements within valley fills are classified in terms of two alternative schemes (Table 2). Scheme 1 (Fig. 2A) classifies the elements on their interpreted (sub-) environment of deposition. Based on the interpretations given in the original work, architectural elements within valley fills are classified as fluvial deposits, non-bay delta, bayhead delta, estuarine bay/lagoon, barrier complex, tidal sand-bar complex, tidal-flat/-channel deposits, near-shore deposits and open-shelf deposits. The non-bay delta environment is defined as a deltaic system that is not fully contained within the confines of the embayment resulting from valley topography (Fig. 2B); only the parts of non-bay delta deposits that infill the incised valleys are considered in the analyses. The barrier complex sub-environment is

Table 2
Schemes adopted for the classification of architectural elements within incised-valley fills.

Scheme 1		Scheme 2	
fluvial deposits	Fluvial channel and floodplain deposits.	fluvial	Products of deposition dominated by river currents.
non-bay delta	A deltaic system that is not fully contained within the confines of the embayment resulting from valley topography. Its delta top sits at higher elevation than the valley interfluves, which are locally buried by the delta, and it infills some relict valley topography during late TST or HST.	wave	Products of deposition dominated by wave action.
bayhead delta	Delta at the head of an estuarine bay or lagoon into which a river discharges.	tide	Products of deposition dominated by tidal currents.
estuarine bay/lagoon	The transition zone between the riverine and the marine environment, where fresh and salt water mix (cf. Allen, 1991), dominated by clay flocculation. It corresponds to 'central basin' environment of Dalrymple et al. (1992).		
barrier complex	Preserved product of a dynamic set of contiguous environments related to barriers or spits (sandy islands above high tide, parallel to the shore, and separated from the coastal plain by a lagoon or bay), such as tidal inlets, washovers, flood-tidal deltas (Dalrymple et al., 1992; Zaitlin et al. 1994; Masselink and Hughes, 2003).		
tidal sand-bar complex	Preserved product of the evolution of a field of tidal bars (Olariu et al., 2012), which are commonly formed within a tide-dominated estuary (e.g., Dalrymple and Zaitlin, 1994; Fenies and Tastet, 1998; Dalrymple et al., 2003) or on the open shelf (e.g., Houbolt, 1968; Berné et al., 2002).		
tidal flat and tidal channel nearshore	Preserved product of deposition in areas of low relief that are alternately exposed and inundated by astronomical tides (cf. Schwartz, 2005), traversed by tidal channels. Bathymetric tract comprised between mean fairweather wave base and mean high water. It includes 'shoreface' and 'foreshore' environments of Reading and Collinson (1996).		
open shelf deposits	Bathymetric tract comprised below the mean fairweather wave base, down to the shelf break. It includes 'offshore transition' and 'offshore' environments of Reading and Collinson (1996).		

defined as the preserved product of a dynamic set of barrier-island environments formed by wave and tidal action, such as tidal inlets, washovers, and flood-tidal deltas; this class includes both spits and barriers (Dalrymple et al., 1992; Dalrymple and Zaitlin, 1994; Masselink and Hughes, 2003). In Scheme 2 architectural elements are classified according to the dominant process regime they record, as

interpreted in the original source work; in-valley architectural elements are classified as fluvial-, wave- or tide-dominated deposits. In some cases, certain deposits (e.g., worm-tube reef, prograding wedge) cannot be classified according to these schemes. However, the schemes (Table 2) encompass the fundamental architectural-element types associated with incised-valley fills and can be applied in parallel. For

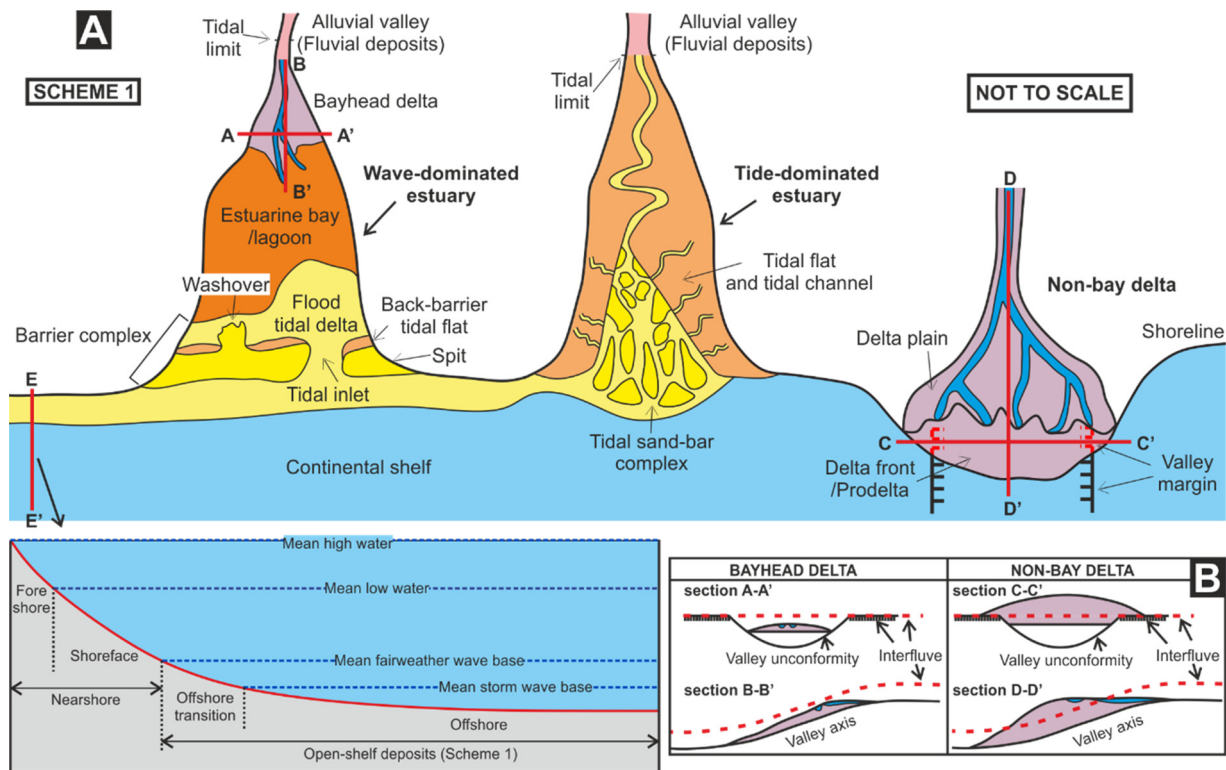


Fig. 2. Definition sketch (A) illustrating the classification of in-valley architectural elements by (sub-)environment of deposition used in this work. Modified from Dalrymple et al. (1992). Inset sketch B depicts idealized sections illustrating the difference between bayhead delta and non-bay delta architectural elements, as defined in this work, and as would be seen along strike and dip orientations. Non-bay deltas are defined as deltaic systems that are not fully contained within the confines of the embayment resulting from valley topography; their delta top sits at higher elevation than the valley interfluves, and they infill some relict valley topography during late TST or HST.

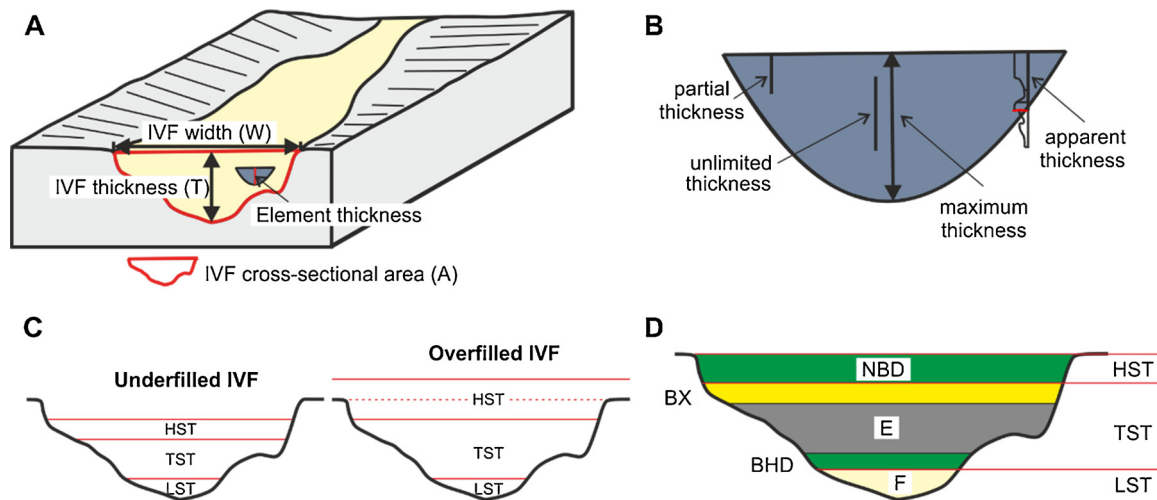


Fig. 3. (A) Incised-valley-fill dimensions (thickness, width and cross-sectional area) and in-valley architectural element thickness measured in the analysis herein. (B) Classification of in-valley architectural element thickness by type of observation, i.e., as ‘maximum’, ‘apparent’, ‘partial’ and ‘unlimited’ (see text). (C) Schematic diagrams illustrating the internal fills for underfilled and overfilled incised valleys (Simms et al., 2006). (D) Diagram illustrating the containment of systems tracts in valley fills, of architectural elements in different systems tracts and of architectural elements in valley fills. For presentation purposes, architectural elements are only shown as classified on Scheme 1; the same elements can also be classified according to Scheme 2. F = fluvial deposits; BHD = bayhead delta; E = estuarine bay/lagoon deposits; BX = barrier complex; NBD = non-bay delta.

scopes of analysis and establishment of an audit trail, the classes of deposits and nomenclatures adopted in the primary data sources are also recorded, though these are not used in the presentation of the results.

2.3. Architectural-element geometry and proportion

In SMAKS, incised-valley fills are themselves recorded as higher-order architectural elements, which act as parent elements to those that form their infills, i.e., their hierarchal containment is tracked (Colombera et al., 2016). The measurement of their geometry (Fig. 3A) follows the approach used by Wang et al. (2019). Incised-valley-fill thickness is defined as the vertical distance between the valley bottom, where deepest, and the top of the valley fill or (for underfilled valleys) the elevation of the interfluves at the valley margins. The term ‘thickness’ is also used to describe the total vertical extent of underfilled valleys because this parameter is always analysed jointly with the thickness of filled valleys. The valley-fill width is defined as the horizontal distance between the valley walls, measured perpendicularly to the valley axis. The valley-fill cross-sectional area is defined as the vertical cross-sectional area subtended by the valley base and either the top of the valley fill or the elevation of interfluves (for underfilled valleys), measured in an orientation perpendicular to the valley axis. The only geometrical parameter analysed in this study for in-valley architectural elements is the thickness. Where the 3D geometry of a certain element is well-constrained (e.g., in high-resolution seismic data), the largest value of thickness of the element along the valley reach is taken, otherwise the largest value of thickness in the studied sample is recorded. Where it is unknown whether the maximum element thickness is observed (e.g., in a 1D core or well-log sample), the thickness is reported as ‘apparent’. Where the base or top of a certain element, or both, are not seen, the thickness is reported as ‘partial’ or ‘unlimited’ (*sensu* Geehan and Underwood, 1993; Fig. 3B), respectively. In statistical analyses of architectural-element thicknesses, only maximum values are used: apparent, partial and unlimited observations are only used for computing element proportions. However, even for this purpose the use of incomplete thicknesses can introduce error to the estimations, since certain deposits might preferentially occur at lower stratigraphic levels, which are commonly undersampled.

Based on their position, architectural elements that form the

incised-valley fills are classified as located beneath present-day coastal plains or on shelves. The relative proportion of architectural elements preserved in different systems tracts within valley fills has been computed based on the sum of their thickness in each systems tracts (Fig. 3D). Similarly, the relative proportion of architectural elements within valley fills has been computed based on the sum of their thickness within valley fills (Fig. 3D). For overfilled IVFs, only the parts of architectural elements or systems tracts that are contained within the incised valleys are considered in the analyses (Fig. 3C). Element proportions have been computed accounting for the fact that in-valley architectural elements can themselves be nested hierarchically. For example, flood-tidal-delta deposits may be encapsulated in a barrier-complex element, or delta-plain deposits may form parts of a non-bay delta (Fig. 2A). Therefore, elements at different hierarchal levels can be selectively included or excluded depending on whether they are classified according to schemes of interest for the scopes of a particular analysis.

2.4. Attributes on geological boundary conditions

In this work, the datasets are filtered on attributes that describe the continental-margin type, drainage-basin area, incised-valley-fill dimensions, basin physiography and shoreline hydrodynamics. The incised-valley fills are classified on the type of continental margin on which they are hosted. The drainage-basin area is defined as the area of the catchments that fed the incised valley at lowstand, landward of the location where the incised-valley-fill geometry was measured (see Wang et al., 2019, for details).

2.4.1. Basin physiography

According to the morphometric definitions and map of global distribution of enclosed and semi-enclosed seas by Healy and Harada (1991a), the coastal-plain IVFs were classified as located along coastlines that either face enclosed/semi-enclosed seas ($N = 23$) or open oceans ($N = 26$). An enclosed or semi-enclosed sea is defined as a sea that is surrounded by land and that is connected with an ocean or another sea by one or more entrances. For practical purposes, this term is restricted to features identifiable on a world map of scale 1:15 M to 1:25 M. In agreement with Healy and Harada (1991a), certain gulf regions, including the Gulf of Mexico and the Gulf of Thailand, were

classified as enclosed or semi-enclosed seas, whereas others, such as the Bay of Biscay, were classified as open-ocean settings.

The present-day shelf physiography is used as a proxy for the physiography of the shelf through the evolution of the valley fills (cf. Wang et al., 2019). Data on shelf width and shelf-break depth are based on the map by Harris et al. (2014) and the digital bathymetric data from Becker et al. (2009). The shelf gradient was calculated as the mean gradient of the shelf between the present-day shoreline and the shelf break. The database also records whether cross-shelf incised-valley fills are characterized on the inner or on the outer shelf. The distinction between inner and outer shelf being made on bathymetry rather than on process regime: the boundary between inner and outer shelf is arbitrarily placed at the 25-m isobath (cf. Wang et al., 2019).

2.4.2. Present-day shoreline hydrodynamics

Mean tidal range and mean wave height at present-day shorelines have been recorded for incised-valley systems beneath modern coastal plains, utilizing digital data from NOAA (2019) and METOCEAN (2019). Values of mean tidal range and mean wave height may not be representative of those at the position where the geometry and architecture of the IVFs were characterized. The duration of tide and wave measurements varies depending on location. Based on records of mean tidal range and mean wave height at the shoreline, the present-day hydrodynamic regime of the coasts (Fig. 4) was classified as tide-dominated, mixed-energy tide-dominated, mixed-energy wave-dominated, or wave-dominated, according to the classification of Davis and Hayes (1984). Because hydrodynamic conditions will vary significantly through a cycle of relative sea-level change (Nordfjord et al., 2006; Yoshida et al., 2005), this classification is only applied to deposits accumulated during the present-day highstand and incorporated in the HST of the incised-valley fills.

2.5. Statistical analyses

Statistical analyses of database outputs have been performed in

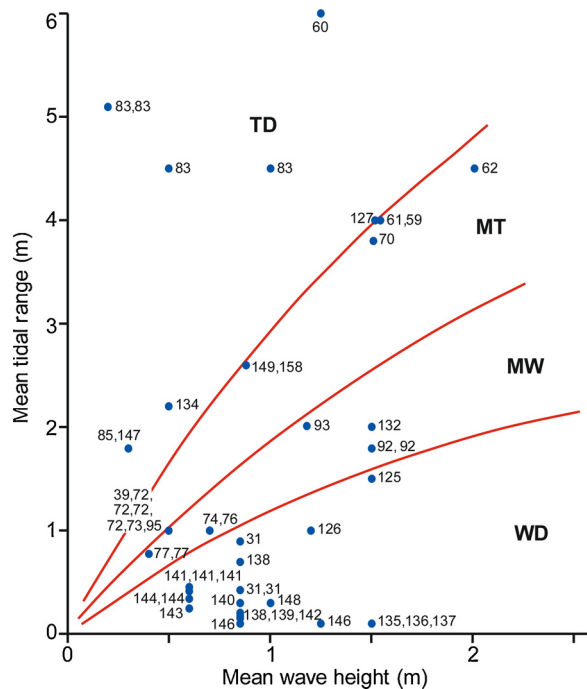


Fig. 4. Plot of mean tidal range versus mean wave height for the present-day shorelines of the studied coastal-plain valleys (cf. Davis and Hayes, 1984). WD = wave-dominated; MW = mixed-energy wave-dominated; MT = mixed-energy tide-dominated; TD = tide-dominated. The numerical labels next to the spots refer to IDs in Table 1. Data from NOAA (2019) and METOCEAN (2019).

Minitab 18 and R (version 3.6.1) (R Core Team, 2019). Statistical analyses have been undertaken to determine relationships between continuous variables and to test hypotheses relating to differences in means or distributions of variables across groups. To quantify linear and monotonic relationships between pairs of continuous variables, Pearson or Spearman correlation coefficients (R and r hereafter) are used respectively; their statistical significance is expressed as P-values (P hereafter). To determine the statistical significance of differences in means across populations, a two-sample *t*-test is used when comparing two sets of observations, whereas one-way analysis of variance (ANOVA) is used when comparing three or more sets of observations. Normality and homoscedasticity of the data were checked before performing these tests, and any variable transformation was applied where needed. The statistical significance of differences across groups, expressed as P-values (P), are determined by resulting test statistics (*t* for *t*-tests, *F* for ANOVA) and the number of degrees of freedom (*df* hereafter). For distributions that are highly skewed and zero-inflated, such as distributions of architectural-element proportions, nonparametric tests are used: the Wilcoxon rank-sum test is used when comparing two sets of observations, whereas the Kruskal-Wallis test is used when dealing with three or more groups. The statistical significance of differences in the distributions across groups is expressed by P-values. P-values are compared with significance levels (α hereafter) that equal 0.05 or 0.1, to determine whether the null hypothesis is rejected.

Additionally, principal component analysis and hierarchical cluster analysis of the variables, were performed on 30 coastal-plain IVFs for which it was possible to constrain the following eight variables: shelf width, shelf-break depth, IVF thickness, IVF width, drainage area, mean wave height, mean tidal range and proportion of fluvial deposits in the valley fills. These multivariate analyses were undertaken for scopes of dimensionality reduction and identification of redundancy across variables. Details, results and discussion of the multivariate analyses are only included in the Supplementary Information.

Further explanation of the statistical methods used can be found in Davis et al. (2002).

2.6. Limitations

Some limitations to the current study that are worth highlighting before any results are presented can be summarized as follows.

- 1 Potential bias exists because of the difficulty in recognizing bounding surfaces in 1D datasets. For example, the thickness and proportion of lowstand fluvial deposits might be over- or underestimated due to the difficulty in recognizing the boundary between lowstand and falling-stage (or older) alluvial units. This type of bias is a significant source of uncertainty in the assessment of variability in the proportion of systems tract or elements for coastal-plain IVFs (section 3.1.1). Additionally, this type of bias might also arise when assessing the difference between the internal fills of coastal-plain incised valleys and cross-shelf incised valleys (section 3.1.2) as the recognition of sequence boundaries relies on different techniques of investigation in onshore versus offshore settings. In seismic sections, where sequence boundaries may be readily apparent, lowstand fluvial deposits tend to be identified more easily, whereas in 1D datasets based on cores or well logs the thickness of lowstand fluvial deposits may be over- or underestimated due to their amalgamation with alluvial deposits of the falling stage or of previous cycles.
- 2 Relationships between direction and magnitude in relative sea-level rise and fall and characteristics of IVF architecture could not be examined in detail. Spatial and temporal variability in sea-level fluctuations are known to exert a control on IVF architecture (Thomas and Anderson, 1994; Nichol et al., 1996; Rodriguez et al., 1999; Hori et al., 2002), and it is therefore likely that some variability in the data presented in this work is related to the temporal change in the rate of post-LGM sea-level rise and fall and to

geographic variations of sea level. Additionally, the valley reaches studied in the original data sources might have been filled under different sea-level conditions depending on their positions relative to the present-day shoreline. A binary distinction between coastal-plain IVFs and cross-shelf IVFs is therefore necessarily simplistic.

- 3 Characteristics relating to the shape of incised valleys and to their variations in shape along their dip extent were not examined. Previous work (Heap and Nichol, 1997; Rodriguez et al., 2005, 2008) has shown that the shape of incised valleys acts as a controlling factor on IVF architecture; for example, the progressive inundation of terraces in terraced IVFs can result in step-wise changes in accommodation space and in variations of hydrodynamic processes, which can influence the valley-fill architecture. It is desirable to attempt further analysis with additional metrics of valley-shape variability along dip to consider its potential control on stratigraphic architectures.
- 4 Factors relating to the morphology of the bedrock that might be exposed along the base of incised valleys and to its potential control on hydrodynamics and resultant sedimentation were not examined.

3. Results

3.1. Valley-fill stratigraphic organization and sea-level control

The sedimentary architecture of incised-valley fills that sit beneath present-day coastal plains and of those that occur on continental shelves are expected to differ, particularly with respect to the extent to which the different systems tracts are preserved in the valley fill, and in the abundance of architectural-element types and its variation through systems tracts (Dalrymple et al., 1992; Allen and Posamentier, 1993, 1994b; Zaitlin et al. 1994; Blum et al., 2013). To assess the significance of these differences, the stratigraphic architecture of coastal-plain (N = 20) and cross-shelf incised-valley fills (N = 18) is considered separately.

3.1.1. Coastal-plain incised valleys

The ratio between the thickness of deposits belonging to a certain systems tract in the valley fill and the thickness of the valley fill itself ('systems tract-to-valley-fill thickness ratio', or simply 'thickness ratio', hereafter) is taken as an estimation of the proportion of the systems tract in the incised-valley fill. The mean thickness ratio (avgTR) of TSTs in incised-valley fills is significantly higher than that of LSTs or HSTs (avgTR_{LST} = 0.18; avgTR_{TST} = 0.62; avgTR_{HST} = 0.20; one-way ANOVA: F(2,57) = 52.42, P-value < 0.001; Fig. 5A). Likewise, the thickness of TSTs within incised-valley fills is, on average, significantly larger than that of LST or HST (avgT_{LST} = 11.8 m; avgT_{TST} = 34.6 m; avgT_{HST} = 11.7 m; one-way ANOVA: F(2,57) = 26.02, P-value < 0.001; Fig. 5B).

For architectural elements accumulated during lowstand times, and which form LSTs in incised-valley fills, fluvial deposits are the most abundant (mean proportion: avgP = 0.98, σ = 0.06; Fig. 5C). In TST valley-fill deposits, estuarine bay/lagoon (avgP = 0.51, σ [standard deviation] = 0.25) deposits are the most abundant type of elements, whereas the second most abundant is represented by fluvial deposits (avgP = 0.20, σ = 0.23). For architectural elements accumulated during highstand times, and which form HSTs, the type with the largest average proportion is represented by non-bay deltas, i.e., deltaic systems that are not fully contained within the confines of the embayment resulting from valley topography, (avgP = 0.29, σ = 0.41); the second most abundant type on average is represented by estuarine bay/lagoon elements (avgP = 0.25, σ = 0.34).

For architectural elements across systems tracts, the mean proportion of fluvial deposits within LST is higher than that within TST or HST (avgP_{LST} = 0.98, σ = 0.06; avgP_{TST} = 0.2, σ = 0.23; avgP_{HST} = 0.06, σ = 0.12; Fig. 5C). The mean proportion of estuarine bay/lagoon elements within TST is higher than that within LST or HST

(avgP_{LST} = 0.00, σ = 0.00; avgP_{TST} = 0.51, σ = 0.25; avgP_{HST} = 0.25, σ = 0.34). When bayhead-delta and non-bay delta units are considered jointly, the mean proportion of these deltaic deposits within HSTs is higher than that within LSTs or TSTs (avgP_{LST} = 0.00, σ = 0.00; avgP_{TST} = 0.09, σ = 0.18; avgP_{HST} = 0.39, σ = 0.38). Differences in the distributions of proportion of fluvial, estuarine bay/lagoon, and deltaic elements across different types of systems tracts are significant at α of 0.05, based on Kruskal-Wallis test (H = 34.69, P-value < 0.001 for fluvial; H = 24.85, P-value < 0.001 for estuarine bay/lagoon elements; H = 13, P-value = 0.002 for deltaic elements).

The thickness of fluvial deposits within TSTs is higher on average than that within LSTs or HSTs (avgT_{LST} = 8.44 m, σ = 7.58 m; avgT_{TST} = 13.12 m, σ = 6.75 m; avgT_{HST} = 6.4 m, σ = 2.29 m; Fig. 5D). Differences in the distributions of thickness of fluvial deposits across systems tracts are significant at α of 0.1 (one-way ANOVA: F(2,50) = 3.09, P-value = 0.055). Differences in the thickness distributions of bayhead delta, estuarine bay/lagoon and barrier-complex elements between TST and HST are not significant, based on two-sample t-tests (t-value = -0.84, P-value = 0.422, df = 10, for bayhead delta; t-value = -1.5, P-value = 0.157, df = 14, for estuarine bay/lagoon; t-value = -0.21, P-value = 0.841, df = 4, for barrier complex).

No significant difference exists between the thickness distributions for incised-valley fills that contain HST deposits compared to those that were overfilled and/or ravined during transgressions and do not contain HST deposits (mean value = 54.2 m versus 50.9 m; σ = 16.2 m versus 24.2 m; two-sample t-test: t-value = 0.28, P-value = 0.788, df = 5).

3.1.2. Cross-shelf incised valleys

For systems tracts within incised-valley fills, the mean systems-tract-to-valley-fill thickness ratio of LSTs or TSTs is significantly higher than that of HSTs (avgTR_{LST} = 0.36; avgTR_{TST} = 0.55; avgTR_{HST} = 0.08; one-way ANOVA: F(2,51) = 24.34, P-value < 0.001; Fig. 6A). The thickness ratio of LST deposits within cross-shelf valley fills is, on average, higher than that within coastal-plain valley fills (avgTR_{shelf} = 0.36; avgTR_{coastal-plain} = 0.18; Fig. 5A and 6 A).

Likewise, the thickness of LSTs or TSTs within incised-valley fills is, on average, significantly larger than that of HST (avgT_{LST} = 13.71 m; avgT_{TST} = 18.95 m; avgT_{HST} = 3.24 m; one-way ANOVA: F(2,51) = 11.53, P-value < 0.001; Fig. 6B).

For architectural elements accumulated during lowstand and that form LSTs in incised-valley fills, fluvial deposits are in almost all cases the only type of deposit (Fig. 6C). For architectural elements accumulated during TST, estuarine-bay/lagoon deposits (avgP = 0.35, σ = 0.40) are the ones with highest average proportion, followed by barrier-complex deposits (avgP = 0.21, σ = 0.32), and tidal-flat and tidal-channel elements (avgP = 0.10, σ = 0.18). For architectural elements accumulated during highstand and that form HSTs, the most abundant element type is open-shelf deposits (avgP = 0.7, σ = 0.48).

The mean proportion of fluvial deposits within LST is higher than that within TST or HST (avgP_{LST} = 1, σ = 0; avgP_{TST} = 0.07, σ = 0.25; avgP_{HST} = 0, σ = 0; Fig. 6C). The mean proportion of estuarine bay/lagoon deposits within TST is higher than that within LST or HST (avgP_{LST} = 0, σ = 0; avgP_{TST} = 0.35, σ = 0.40; avgP_{HST} = 0.1, σ = 0.32). The mean proportion of open-shelf deposits within HST is higher than that within LST or TST (avgP_{LST} = 0, σ = 0; avgP_{TST} = 0.08, σ = 0.24; avgP_{HST} = 0.7, σ = 0.48). Differences in the distributions of proportion of fluvial, estuarine bay/lagoon, and open-shelf deposits across different systems tracts in valley fills are statistically significant at α of 0.05, based on Kruskal-Wallis test (H = 35.92, P-value < 0.001 for fluvial deposits; H = 12.44, P-value = 0.002 for estuarine bay/lagoon; H = 17.17, P-value < 0.001 for open-shelf deposits).

The average thickness of fluvial deposits, i.e., of stratigraphic packages that might variably include fluvial channel and floodplain

Coastal-plain IVFs

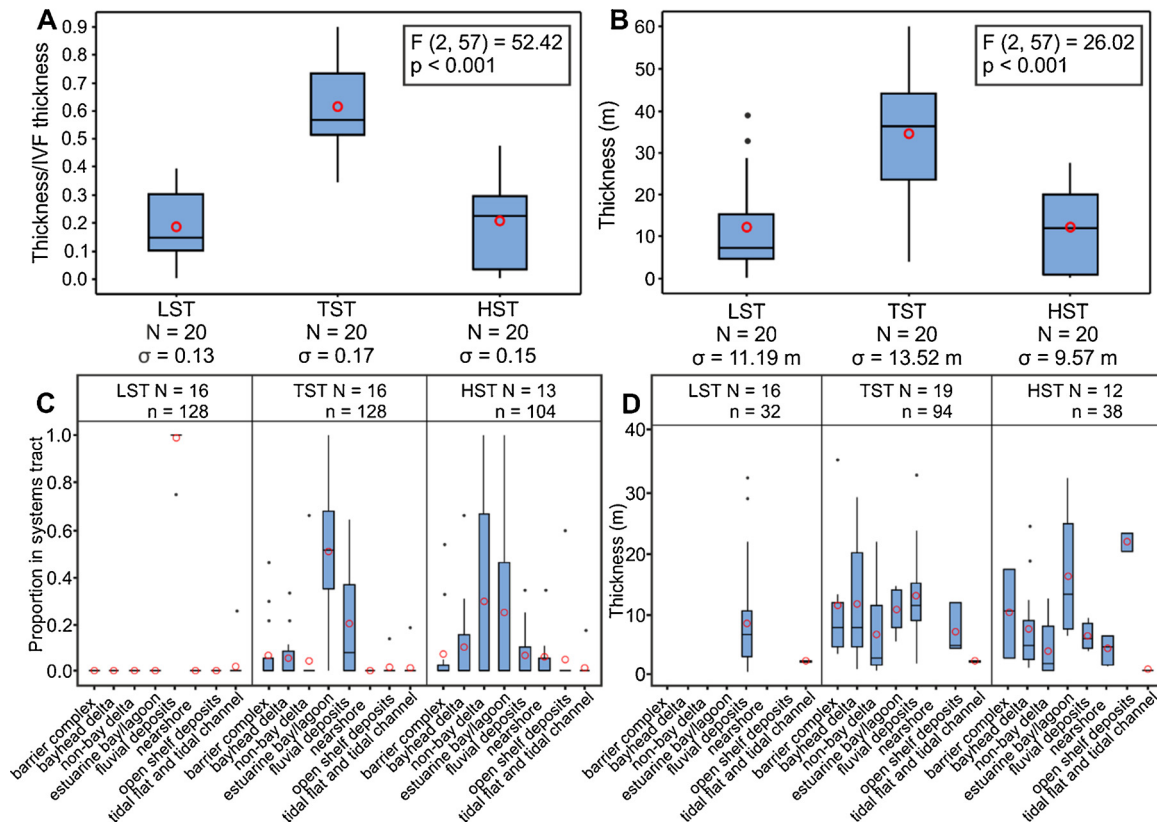


Fig. 5. Box plots that present distributions in: (A) systems-tract-to-valley-fill thickness ratio and (B) thickness of different systems tracts preserved in coastal-plain incised-valley fills; (C) proportion and (D) thickness of architectural elements belonging to each type of systems tract in coastal-plain valley fills. For each box plot, boxes represent interquartile ranges, red open circles represent median values, horizontal bars within the boxes represent median values and black dots represent outliers (values that are more than 1.5 times the interquartile range). 'N' denotes the number of incised-valley fills and associated systems tract, 'n' denotes the number of architectural elements in each systems tract and 'σ' denotes the standard deviation. The results of one-way ANOVA are reported in boxes in parts A and B, as: F-value (degrees of freedom between and within groups in brackets), P-value.

deposits, is not significantly different between LST and TST ($\text{avgT}_{\text{LST}} = 15.3 \text{ m}$ [$\sigma = 11.7 \text{ m}$], $\text{avgT}_{\text{TST}} = 15.8 \text{ m}$ [$\sigma = 1.63 \text{ m}$]; two-sample *t*-test: *t*-value = -0.19 , *P*-value = 0.854 , *df* = 15 ; Fig. 6D). The average thickness of open-shelf deposits is smaller in HST than in TST intervals ($\text{avgT}_{\text{HST}} = 3.7 \text{ m}$ [$\sigma = 1.68 \text{ m}$], $\text{avgT}_{\text{TST}} = 12.7 \text{ m}$ [$\sigma = 11.6 \text{ m}$]); however, these differences are not statistically significant (two-sample *t*-test: *t*-value = -1.55 , *P*-value = 0.218 , *df* = 3).

3.2. Continental-margin type

The mean and median proportions of fluvial deposits within incised-valley fills developed along tectonically active margins are higher than those for valley fills along passive margins (Fig. 7A). A 17% difference in mean proportion of fluvial deposits is seen between active margins and passive margins, for which differences in the distributions are statistically significant at α of 0.05 , based on Wilcoxon rank-sum tests ($W = 242$, *P*-value = 0.007). For incised-valley fills developed along tectonically active margins, the mean proportions of bayhead delta or estuarine bay/lagoon elements appear to be lower than those for valley fills along passive margins. However, differences in the distributions of the proportions of these two types of elements within incised-valley fills across margin types are not statistically significant, based on Wilcoxon rank-sum tests ($W = 154$, *P*-value = 0.721 for bayhead delta; $W = 146$, *P*-value = 0.554 for estuarine bay/lagoon deposits).

Differences in means of the thickness of fluvial, bayhead-delta and barrier-complex elements within valley fills across these two settings are not statistically significant, based on two-sample *t*-tests (*t*-value = 1.04 , *P*-value = 0.307 , *df* = 37 , for fluvial deposits; *t*-value =

-1.16 , *P*-value = 0.265 , *df* = 15 , for bayhead delta; *t*-value = 0.71 , *P*-value = 0.486 , *df* = 19 , for barrier complex; Fig. 7B). The thickness of estuarine bay/lagoon elements within valley fills along active margins is, on average, larger than that within valley fills along passive margins ($\text{avgT}_{\text{active}} = 11.7 \text{ m}$, $\text{avgT}_{\text{passive}} = 6.5 \text{ m}$; two-sample *t*-test: *t*-value = 2.76 , *P*-value = 0.01 , *df* = 29).

3.3. Catchment and basin physiography

3.3.1. Record of systems tracts in incised-valley fills and river-system size

For systems tracts in incised-valley fills, positive correlations are seen between the thickness of LST deposits versus incised-valley-fill thickness, width and cross-sectional area (Fig. 8A–C; Table 3). Positive correlations are also seen between the thickness of TST deposits versus incised-valley-fill thickness and valley drainage-basin area (Fig. 8A and D; Table 3). A modest positive relationship is seen between HST thickness and incised-valley-fill thickness (Fig. 8A; Table 3).

Positive correlations are seen between the LST-to-valley-fill thickness ratio and incised-valley-fill thickness or cross-sectional area (Fig. 8E and G; Table 3). No apparent correlations are seen between thickness ratios of TSTs or HSTs versus incised-valley-fill dimensions or drainage-basin areas (Fig. 8E–H; Table 3).

3.3.2. Architectural elements and river-system size

Relationships between river-system size and the proportion and thickness of architectural elements within valley fills have been investigated, by considering classifications of the elements by sub-environment of deposition (Fig. 9; Table 4) and according to their process

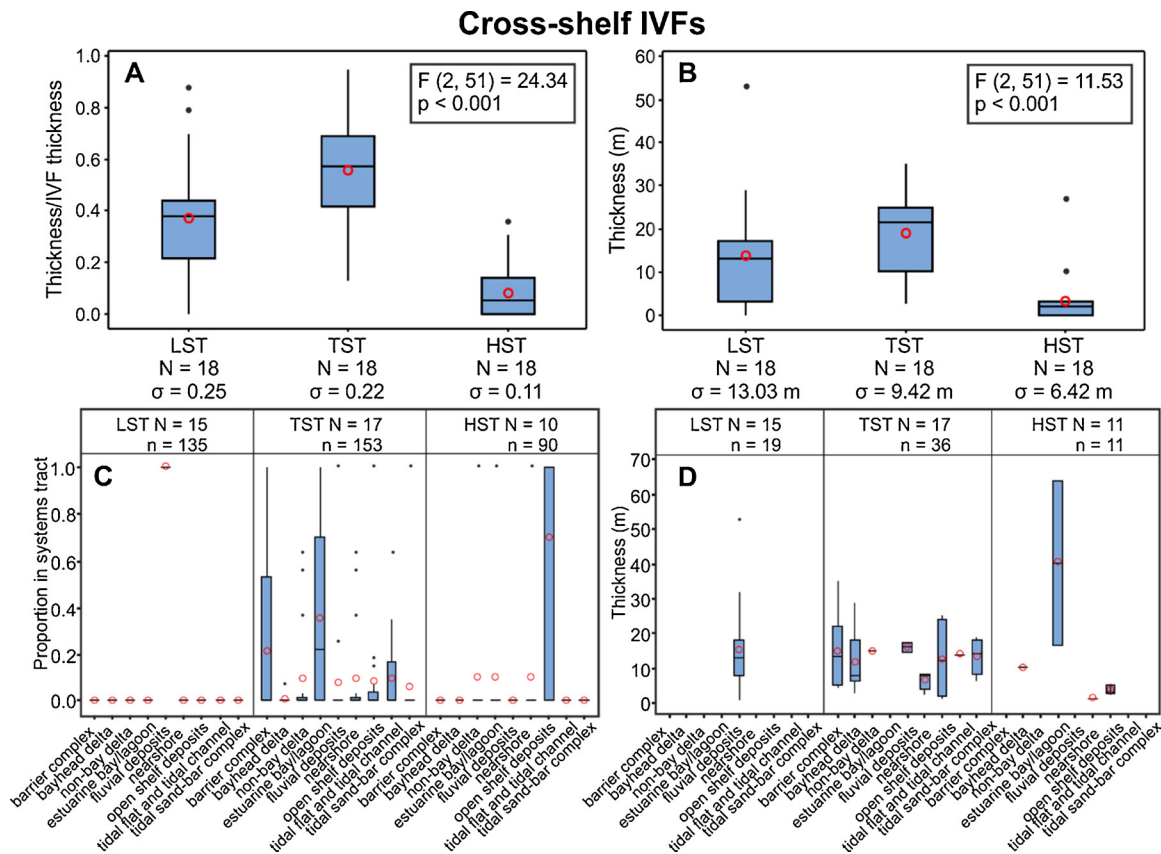


Fig. 6. Box plots that present distributions in: (A) thickness ratio and (B) thickness of different systems tracts preserved in cross-shelf incised-valley fills; (C) proportion and (D) thickness of architectural elements belonging to types of systems tract in cross-shelf valley fills. For each box plot, boxes represent interquartile ranges, red open circles represent mean values, horizontal bars within the boxes represent median values and black dots represent outliers (values that are more than 1.5 times the interquartile range). ‘N’ denotes the number of incised-valley fills and associated systems tract, ‘n’ denotes the number of architectural elements in each systems tract and ‘ σ ’ denotes the standard deviation. The results of one-way ANOVA are reported in boxes in parts A and B, as: F-value (degrees of freedom between and within groups in brackets), P-value.

regime (Fig. 10; Table 5). In these analyses, the size of the valley systems are considered in terms of incised-valley-fill thickness, width, and drainage area (Figs. 9 and 10; Tables 4 and 5).

3.3.3. Process regime, architectural elements and coastal physiography

For coastal-plain IVFs, differences in both present-day processes (mean wave height and mean tidal range at the shoreline) and preserved sedimentary products (proportion of elements recording different process regimes) across enclosed or semi-enclosed sea and open-ocean settings (Fig. 11) are investigated. The mean wave height (avgMWH) for the studied open-ocean settings is, on average, higher than that in enclosed or semi-enclosed seas ($\text{avgMWH}_{\text{open}} = 1.077$ m, $\text{avgMWH}_{\text{enclosed}} = 0.713$ m; two-sample *t*-test: *t*-value = -3.14, *P*-value = 0.004, *df* = 33; Fig. 11A). The mean tidal range (avgTR) in the studied open-ocean settings is, on average, higher than that in enclosed or semi-enclosed seas ($\text{avgTR}_{\text{open}} = 1.48$ m, $\text{avgTR}_{\text{enclosed}} = 0.640$ m; two-sample *t*-test: *t*-value = -2.41, *P*-value = 0.022, *df* = 29; Fig. 11B).

The mean proportion of wave-dominated elements in IVFs facing enclosed or semi-enclosed seas is marginally lower than that for IVFs associated with open oceans ($\text{avgP}_{\text{enclosed}} = 0.231$ vs $\text{avgP}_{\text{open}} = 0.287$), though to a level that is not statistically significant (two-sample *t*-test: *t*-value = -0.65, *P*-value = 0.522, *df* = 45). The proportion of tide-dominated elements in IVFs associated with enclosed or semi-enclosed seas is, on average, significantly lower than that for IVFs associated with open oceans ($\text{avgP}_{\text{enclosed}} = 0.051$ vs $\text{avgP}_{\text{open}} = 0.315$; two-sample *t*-test: *t*-value = -3.87, *P*-value < 0.001, *df* = 33). The mean proportion of fluvial-dominated elements in IVFs associated with enclosed or semi-enclosed seas is significantly higher

than that for IVFs facing open oceans ($\text{avgP}_{\text{enclosed}} = 0.718$ vs $\text{avgP}_{\text{open}} = 0.399$; two-sample *t*-test: two-sample *t*-test: *t*-value = 3.54, *P*-value = 0.001, *df* = 44).

3.3.4. Process regime, architectural elements and shelf physiography

For coastal-plain IVFs, relationships between shelf physiography (shelf width, shelf-break depth and shelf gradient) and present-day hydrodynamic conditions (Table 6) are investigated. A modest positive correlation is noted between mean wave height at the present-day shoreline at the IVF location versus shelf-break depth. Relationships between shelf physiography and the proportion in coastal-plain IVFs of architectural elements classified according to their dominant process regime (Table 6) are also investigated. A modest positive correlation is noted between the proportion of wave-dominated elements in IVFs versus the average shelf gradient.

3.3.5. Sub-environments of architectural elements and shelf gradient

For incised-valley fills hosted on the outer shelf, positive correlations are seen between the average shelf gradient and both the thickness and proportion of barrier-complex elements (Fig. 12; Table 7).

For incised-valley fills hosted on the shelf, no correlation is noted between the thickness of estuarine bay/lagoon elements versus the average shelf gradient (Fig. 12A; Table 7); a modest positive correlation is noted between the proportion of estuarine bay/lagoon elements versus the average shelf gradient (Fig. 12B; Table 7).

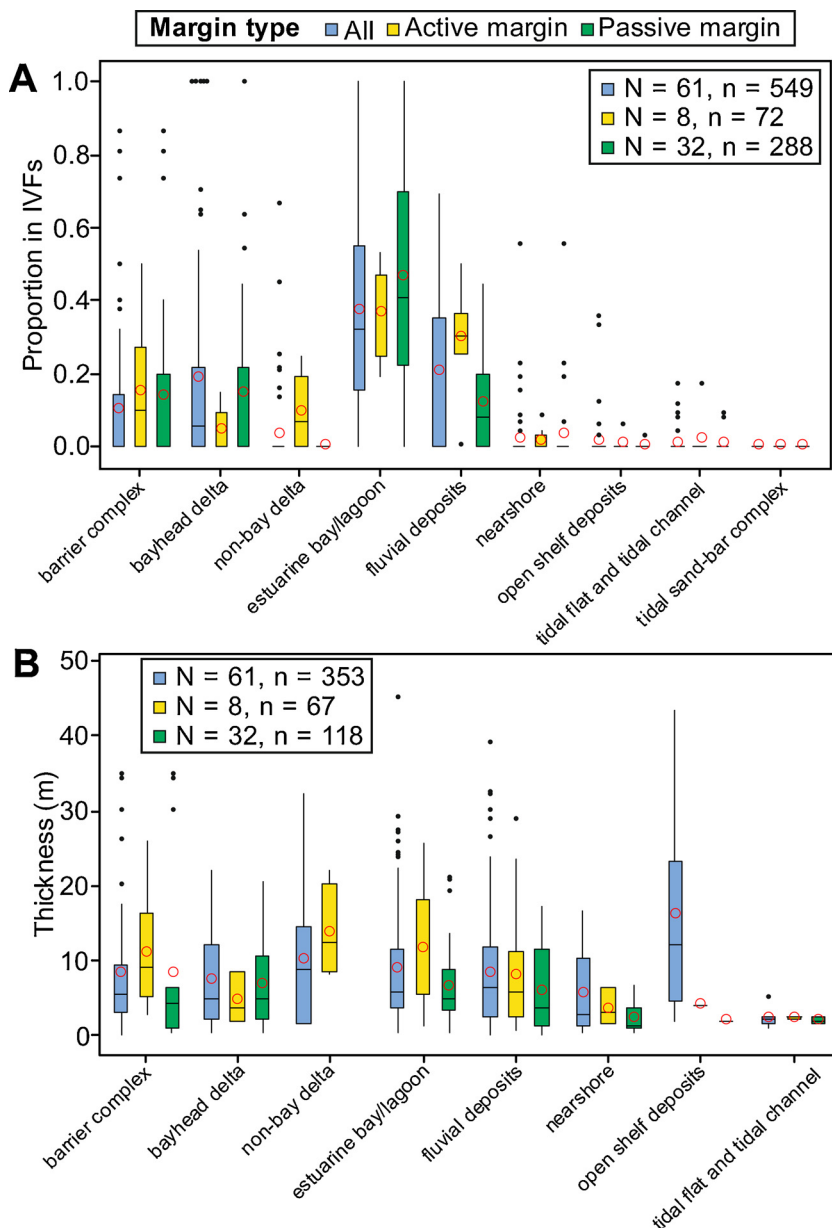


Fig. 7. Box plots that present distributions in: (A) proportion and (B) thickness of different architectural-element types within coastal-plain incised-valley fills; data are presented for all the examples, and separately for active and passive continental margins. For each box plot, boxes represent interquartile ranges, red open circles represent mean values, horizontal bars within the boxes represent median values and black dots represent outliers (values that are more than 1.5 times the interquartile range). 'N' denotes the number of incised-valley fills associated with each margin type and 'n' denotes the number of corresponding in-valley architectural elements.

3.4. Shoreline hydrodynamics

Previous work based on late-Quaternary incised-valley-fill systems and outcrop studies of ancient successions (e.g., Yoshida et al., 2005; Nordfjord et al., 2006; Tanabe et al., 2006) has demonstrated that hydrodynamic conditions through a relative sea-level cycle change in response to several factors, such as wind regime, coastal bathymetry, shelf-break depth, shelf width, their effect on tidal resonance, and frictional forces. To investigate the relationships between coastal hydrodynamics and resultant sedimentary record, this work only focuses on deposits accumulated during highstand and incorporated in the HST of incised-valley fills, by considering the present-day hydrodynamic regimes at the respective shorelines. The following observations (Fig. 13) are based on a limited dataset ($N = 19$) and thus any relationships between hydrodynamics and highstand deposits in incised-valley fills needs to be substantiated with more data.

For deposits accumulated during highstand and forming HSTs within coastal-plain incised-valley fills (Fig. 13A), the thickness ratio of HSTs in valley fills associated with present-day mixed-energy to fully wave-dominated conditions is smaller on average compared to that of

valley fills associated with present-day fully tide-dominated conditions or mixed-energy tide-dominated conditions ($\text{avgTR}_{\text{HST-MW/WD}} = 0.18$; $\text{avgTR}_{\text{HST-TD}} = 0.26$; $\text{avgTR}_{\text{HST-MT}} = 0.26$); differences in mean values of the thickness ratio of HSTs in valley fills across different present-day hydrodynamic regimes are not statistically significant (one-way ANOVA: $F(2,16) = 0.52$, $P\text{-value} = 0.602$).

For architectural elements accumulated during the highstand and forming HSTs within incised-valley fills, the proportion of tide-dominated elements is on average higher in incised-valley fills associated with present-day tide-dominated conditions (e.g., Palaeo-Arakawa valley, Palaeo-Nakagawa valley, Palaeo-Tokyo valley in Japan; Qiantang valley in China) or mixed-energy tide-dominated conditions (e.g., Gironde estuary in France), compared to valley fills associated with increased dominance of wave processes ($\text{avgP}_{\text{TD}} = 0.73$; $\text{avgP}_{\text{MT}} = 0.60$; $\text{avgP}_{\text{MW/WD}} = 0.00$ Fig. 13B). For example, according to the classification of Davis and Hayes (1984), the Qiantang incised valley (China; case study 83 in Table 1), now a drowned-valley estuary, is currently subject to tide-dominated conditions at the modern shoreline. The HST of the valley fills is characterized by a tide-dominated estuary that contains a tidal sand-bar complex. In the HSTs of incised-

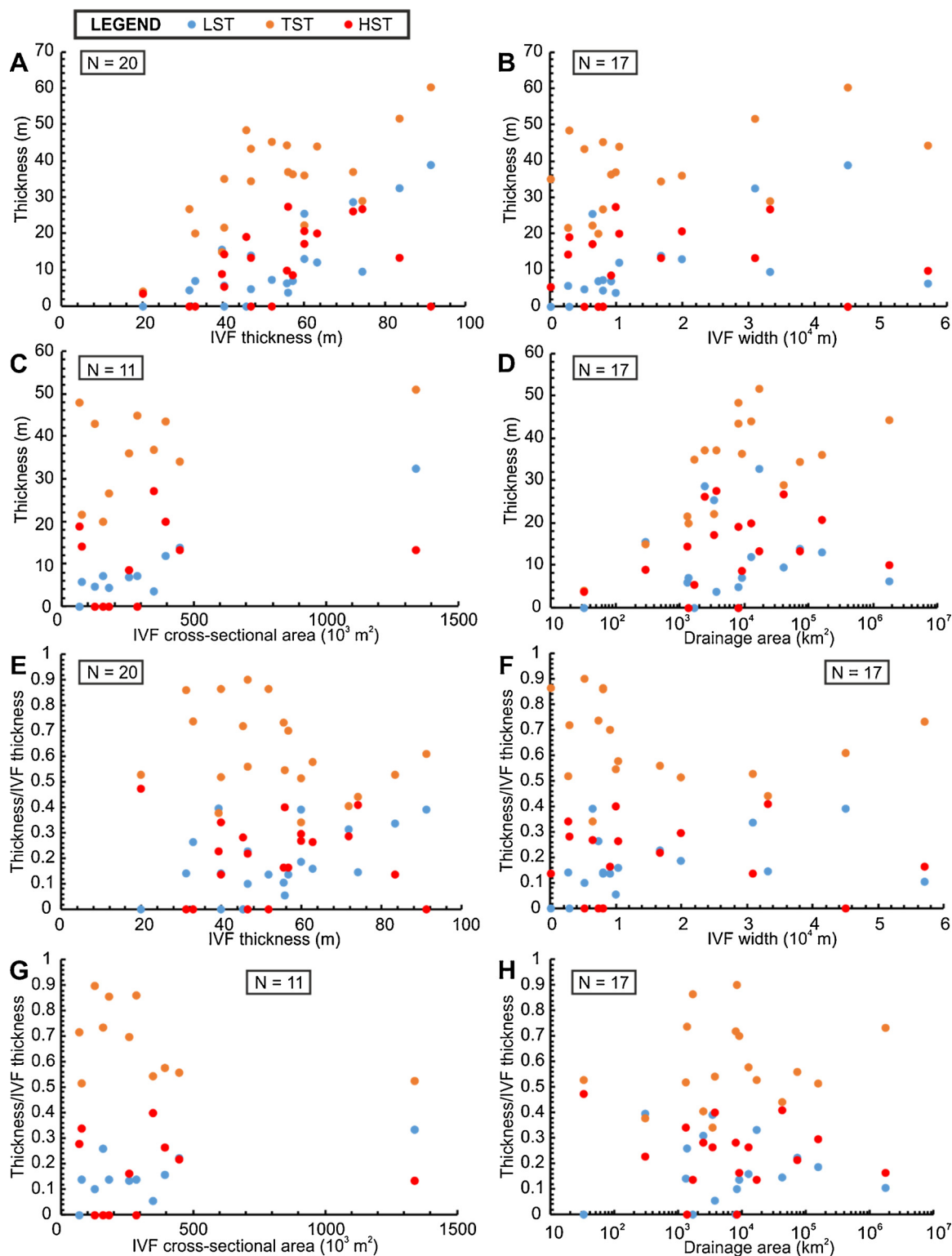


Fig. 8. Cross-plots of the thickness of systems tracts within coastal-plain incised-valley fills versus IVF thickness (A), width (B), cross-sectional area (C) and drainage-basin area (D). Cross-plots of the thickness ratio of systems tracts within coastal-plain incised-valley fills versus IVF thickness (E), width (F), cross-sectional area (G) and drainage-basin area (H). For each pair of variables, the correlation coefficients and P-values are reported in Table 3. ‘N’ denotes the number of incised-valley fills.

valley fills associated with present-day mixed-energy to fully wave-dominated conditions, the proportion of wave-dominated elements is on average higher compared to that in valley-fills associated with present-day fully tide-dominated conditions or mixed-energy tide-dominated conditions ($avgP_{MW/WD} = 0.86$; $avgP_{MT} = 0.17$; $avgP_{TD} = 0.08$).

For coastal-plain incised valleys, relationships are also investigated between valley-fill width and present-day hydrodynamic regimes (Fig. 14). A positive correlation is seen between incised-valley-fill width versus present-day mean tidal range at the shoreline ($r = 0.654$, P-value < 0.001; Fig. 14A). A very weak negative correlation is seen between incised-valley-fill width versus present-day mean wave height

Table 3
Correlation coefficients and P-values reported for the relationship between the thickness or thickness ratio of systems tracts within coastal-plain incised-valley fills versus IVF thickness, IVF width, IVF cross-sectional area and drainage area. 'N' denotes the number of readings, 'R' denotes Pearson's R, and 'r' denotes Spearman's rho.

Parameters	Systems tract	IVF thickness	IVF width	IVF cross-sectional area	Drainage area
Thickness	LST	N = 20; R = 0.774, p < 0.001; r = 0.666, p = 0.001	N = 17; R = 0.498, p = 0.042; r = 0.596, p = 0.012	N = 11; R = 0.958, p < 0.001; r = 0.727, p = 0.011	N = 17; R = -0.111, p = 0.671; r = 0.258, p = 0.317
	TST	N = 20; R = 0.700, p = 0.001; r = 0.611, p = 0.004	N = 17; R = 0.456, p = 0.065; r = 0.380, p = 0.133	N = 11; R = 0.490, p = 0.126; r = 0.291, p = 0.385	N = 17; R = 0.243, p = 0.347; r = 0.613, p = 0.009
	HST	N = 20; R = 0.391, p = 0.089; r = 0.450, p = 0.047	N = 17; R = 0.050, p = 0.849; r = 0.191, p = 0.463	N = 11; R = 0.204, p = 0.547; r = 0.191, p = 0.574	N = 17; R = -0.086, p = 0.744; r = 0.336, p = 0.187
Thickness ratio	LST	N = 20; R = 0.498, p = 0.026; r = 0.411, p = 0.071	N = 17; R = 0.345, p = 0.175; r = 0.441, p = 0.076	N = 11; R = 0.690, p = 0.019; r = 0.536, p = 0.089	N = 17; R = -0.132, p = 0.612; r = 0.147, p = 0.572
	TST	N = 20; R = -0.329, p = 0.157; r = -0.30, p = 0.169	N = 17; R = -0.226, p = 0.384; r = -0.350, p = 0.168	N = 11; R = -0.454, p = 0.160; r = -0.364, p = 0.272	N = 17; R = 0.213, p = 0.412; r = 0.111, p = 0.672
	HST	N = 20; R = -0.055, p = 0.819; r = 0.086, p = 0.717	N = 17; R = -0.025, p = 0.925; r = 0.104, p = 0.691	N = 11; R = 0.011, p = 0.973; r = 0.014, p = 0.968	N = 17; R = -0.133, p = 0.610; r = -0.099, p = 0.706

at the shoreline ($r = -0.256$, $P\text{-value} = 0.111$; Fig. 14B). The width of valley fills in tide-dominated or mixed-energy tide-dominated conditions is on average higher than that associated with valley fills in mixed-energy wave-dominated or fully wave-dominated conditions ($\text{avg}W_{TD} = 27,511$ m; $\text{avg}W_{MT} = 22,247$ m; $\text{avg}W_{MW} = 10,968$ m; $\text{avg}W_{WD} = 4556$ m; Fig. 14C); differences in mean values of incised-valley-fill width across different present-day hydrodynamic regimes are statistically significant (one-way ANOVA: $F(3,29) = 7.24$, $P\text{-value} = 0.001$).

4. Discussion

4.1. Comparison with previously published models

A comparison of the studied late-Quaternary examples with generic facies models for incised-valley fills (e.g., Dalrymple et al., 1992; Zaitlin et al. 1994) and with a model proposed for the Gironde estuary in France (Allen and Posamentier, 1994b) highlights what aspects of the models are, or are not, supported by observations in late-Quaternary examples.

In both the coastal-plain and cross-shelf incised-valley fills studied in this work, the TST represents the largest part of the fills (Fig. 5A and 6 A). Coastal-plain valley fills (cf. the 'middle segment' in Zaitlin et al. 1994) are typically characterized by fluvial deposits in LSTs and estuarine bay/lagoon deposits in TSTs, capped by non-bay deltaic deposits or bayhead delta deposits in HSTs (Fig. 5). Cross-shelf valley fills (cf. the 'outer segment' in Zaitlin et al. 1994) are typically characterized by fluvial deposits in LSTs and estuarine bay/lagoon deposits in TSTs, capped by condensed open-shelf deposits in HSTs (Fig. 5). Observations of stratigraphic organization in the studied late-Quaternary examples support the classical facies models for incised-valley fills as a representative base case (Dalrymple et al., 1992; Zaitlin et al. 1994; Allen and Posamentier, 1994b).

However, the internal fills of valleys incised into modern shelves display significant variability in facies architecture (Fig. 15C; cf. Chaumillon et al., 2008) and differ in two ways from the studied coastal-plain valleys and from what is represented in the models.

First, the studied cross-shelf incised-valley fills are characterized by a higher proportion of lowstand deposits, compared to the studied coastal-plain valley fills (Fig. 5A and 6 A). Specifically, in the palaeo-Chao Praya valleys (Case study 67, Table 1; Reijenstein et al., 2011) on the Sunda shelf, LST fluvial deposits make up the largest portion of the valley fills, and are only capped by relatively thin TST estuarine mud deposits. In the Changjiang-Qiangtangjiang incised valley of the East China Sea shelf (Case study 83 in Table 1; Wellner and Bartek, 2003), LST fluvial deposits represent the largest part of the valley fills, capped by limited HST tidal-bar complex deposits. Transgression within this valley fill is only recorded by ravinement. These characteristics also contrast with the limited LST fluvial deposits depicted in existing models for the seaward portion of incised-valley fills (Zaitlin et al. 1994; Allen and Posamentier, 1994b). There may be two reasons for this difference. Firstly, some of the valleys in this study are fed by large river systems, with extensive catchments arising from the amalgamation of the drainage areas of rivers that join on the shelf. Thus, these large rivers, which are associated with large drainage areas and maximum bankfull depths, can generate thicker channel belts, bars and channel fills (Fielding and Crane, 1987; Bridge and Mackey, 1993; Shanley, 2004; Fielding et al., 2006; Gibling, 2006; Blum et al., 2013); this, in turn, can translate to thicker LST fluvial deposits within valley fills. Furthermore, the gradient of shelves that occur offshore of river-dominated coasts is in part determined by the profile of the rivers traversing it at lowstand, and larger fluvial systems are associated with lower channel gradients (Wood et al., 1993; Burgess et al., 2008; Blum and Womack, 2009; Olariu and Steel, 2009; Sømme et al., 2009a, 2009b; Helland-Hansen et al., 2012; Blum et al., 2013). Thus, larger valleys, being fed by larger river systems, are generally associated with

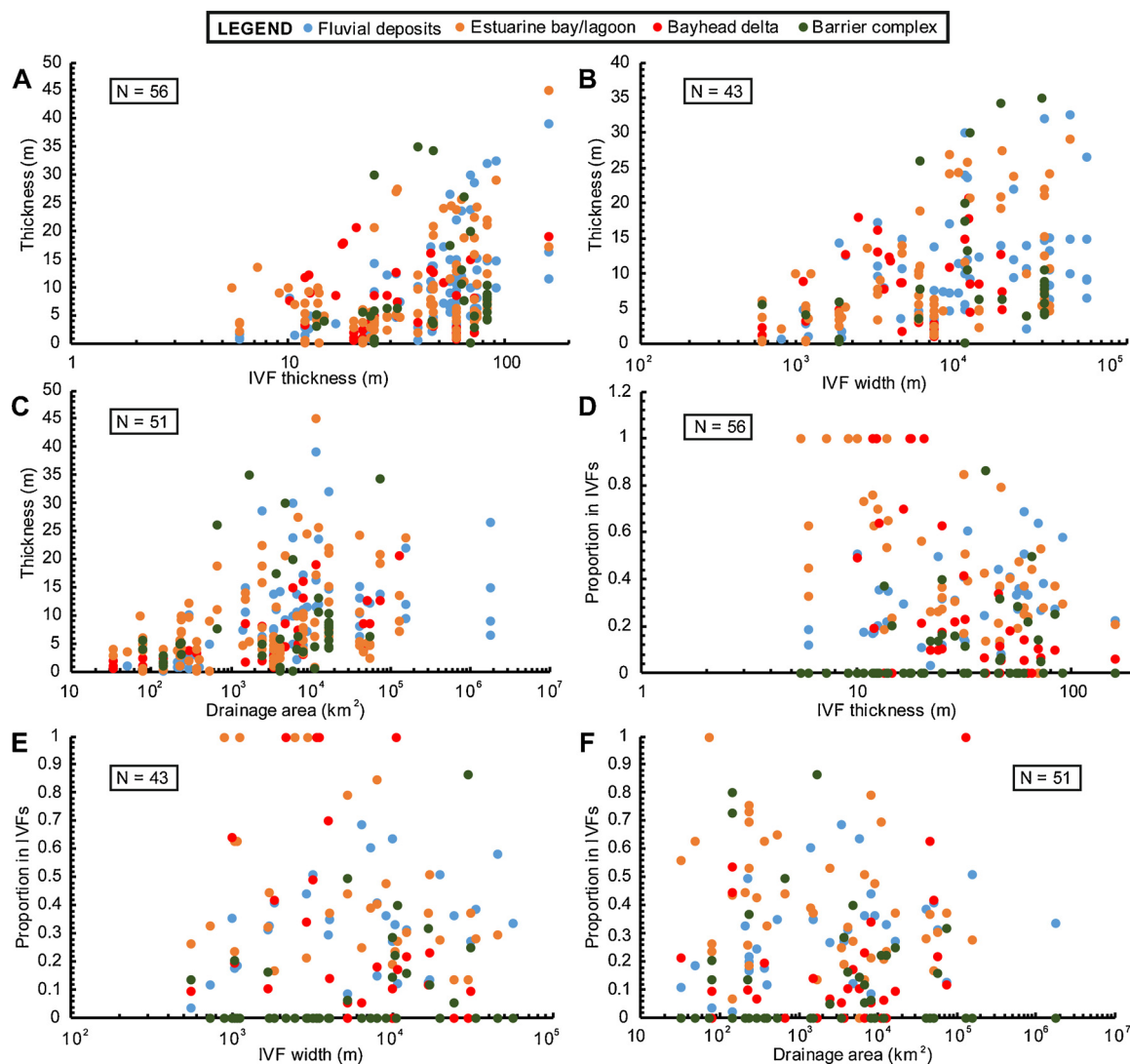


Fig. 9. Cross-plots of thickness of architectural elements within coastal-plain incised-valley fills versus IVF thickness (A), width (B) and drainage-basin area (C). Cross-plots of proportion of architectural elements within coastal-plain incised-valley fills versus IVF thickness (D), width (E) and drainage-basin area (F). Architectural elements are classified on their sub-environment of deposition. For each pair of variables, the correlation coefficients and P-values are reported in respective cell in Table 4. 'N' denotes the number of incised-valley fills.

lower-gradient shelves on which the shoreline can migrate rapidly in response to transgression. This could cause any high-energy environment (wave and/or tide dominated environment) at the shoreline to rapidly backstep along the path of extant cross-shelf incised valleys, therefore minimizing the impact of potential erosion of fluvial deposits.

Second, compared to the studied coastal-plain examples, the studied cross-shelf incised-valley fills are characterized by a higher proportion of shelf deposits (Fig. 5A and 6 A). Some incised valleys hosted on the shelf had not yet been filled completely by sediments when the transgressive shoreline backstepped over them, or were excavated again during transgression, leading to the filling of the relict accommodation with open-marine deposits (Simms et al., 2010). Depending on the dominant shelf process responsible for filling the valley, the nature of the infills of these valleys (Fig. 15C) can vary, and can include, for instance, the preserved products of shelf dunes (Case study 49 in Table 1; Payenberg et al., 2006), of sediment gravity flows (Thieler et al., 2007), or offshore muds (Case study 67 in Table 1; Reijenstein et al., 2011). Specifically, the incised-valley fill hosted on the outer shelf in Hervey Bay, on the Pacific coast of Australia (Case study 49 in Table 1; Payenberg et al., 2006), is thought to be entirely filled by the deposits of shelf sand dunes, developed under the influence of strong

tidal currents prevailing on the modern shelf. This valley fill is distinctively different from the fluvial- to estuarine-filled system presented by the general valley-fill models for the seaward portion of incised valleys (Dalrymple et al., 1992; Dalrymple and Zaitlin, 1994; Allen and Posamentier, 1994b).

The general stratigraphic organization of the studied incised-valley fills is consistent with what is depicted qualitatively in classical facies models (e.g., Dalrymple et al., 1992; Zaitlin et al. 1994; Allen and Posamentier, 1994b), which reflect the primary control of sea level. However, overall, based on a large composite dataset, this synthesis demonstrates the internal fills of incised valleys are characterized by significant variability in stratigraphic architectures (Fig. 15; cf. Chaumillon et al., 2008, 2010), which is not accounted for by these models. Variations in the facies architecture of coastal-plain and cross-shelf valley fills can be attributed to controls other than relative sea-level change, such as tectonic setting (continental-margin type), basin physiography, catchment area, river-system size and shoreline hydrodynamics. In the following section, these controls are discussed in detail.

Table 4

Correlation coefficients and P-values reported for the relationship between the thickness or proportion of fluvial deposits, estuarine bay/lagoon, bayhead delta and barrier complex elements within IVFs versus IVF thickness, IVF width and drainage area. 'N' denotes the number of readings, 'R' denotes Pearson's R, and 'r' denotes Spearman's rho.

Parameters	Elements	IVF thickness	IVF width	Drainage area
Thickness	Fluvial deposits	N = 56; R = 0.508, p < 0.001; r = 0.458, p < 0.001	N = 43; R = 0.406, p < 0.001; r = 0.529, p < 0.001	N = 51; R = 0.171, p = 0.090; r = 0.691, p < 0.001
	Estuarine bay/lagoon	N = 56; R = 0.517, p = 0.001; r = 0.420, p < 0.001	N = 43; R = 0.454, p < 0.001; r = 0.524, p < 0.001	N = 51; R = 0.220, p = 0.027; r = 0.351, p < 0.001
	Bayhead delta	N = 56; R = 0.230, p = 0.144; r = 0.017, p = 0.915	N = 43; R = 0.390, p = 0.027; r = 0.225, p = 0.216	N = 51; R = 0.550, p < 0.001; r = 0.782, p < 0.001
	Barrier complex	N = 56; R = 0.047, p = 0.797; r = 0.242, p = 0.175	N = 43; R = 0.112, p = 0.570; r = 0.324, p = 0.093	N = 51; R = 0.314, p = 0.055; r = 0.318, p = 0.052
Proportion	Fluvial deposits	N = 56; R = 0.412, p = 0.002; r = 0.473, p < 0.001	N = 43; R = 0.264, p = 0.088; r = 0.273, p = 0.077	N = 51; R = 0.082, p = 0.570; r = 0.237, p = 0.094
	Estuarine bay/lagoon	N = 56; R = -0.243, p = 0.071; r = -0.24, p = 0.059	N = 43; R = -0.238, p = 0.125; r = -0.191, p = 0.220	N = 51; R = -0.175, p = 0.219; r = -0.113, p = 0.430
	Bayhead delta	N = 56; R = -0.242, p = 0.072; r = 0.014, p = 0.918	N = 43; R = -0.235, p = 0.129; r = -0.103, p = 0.511	N = 51; R = -0.039, p = 0.785; r = 0.126, p = 0.379
	Barrier complex	N = 56; R = 0.399, p = 0.002; r = 0.354, p = 0.007	N = 43; R = 0.335, p = 0.028; r = 0.299, p = 0.051	N = 51; R = 0.082, p = 0.566; r = -0.017, p = 0.907

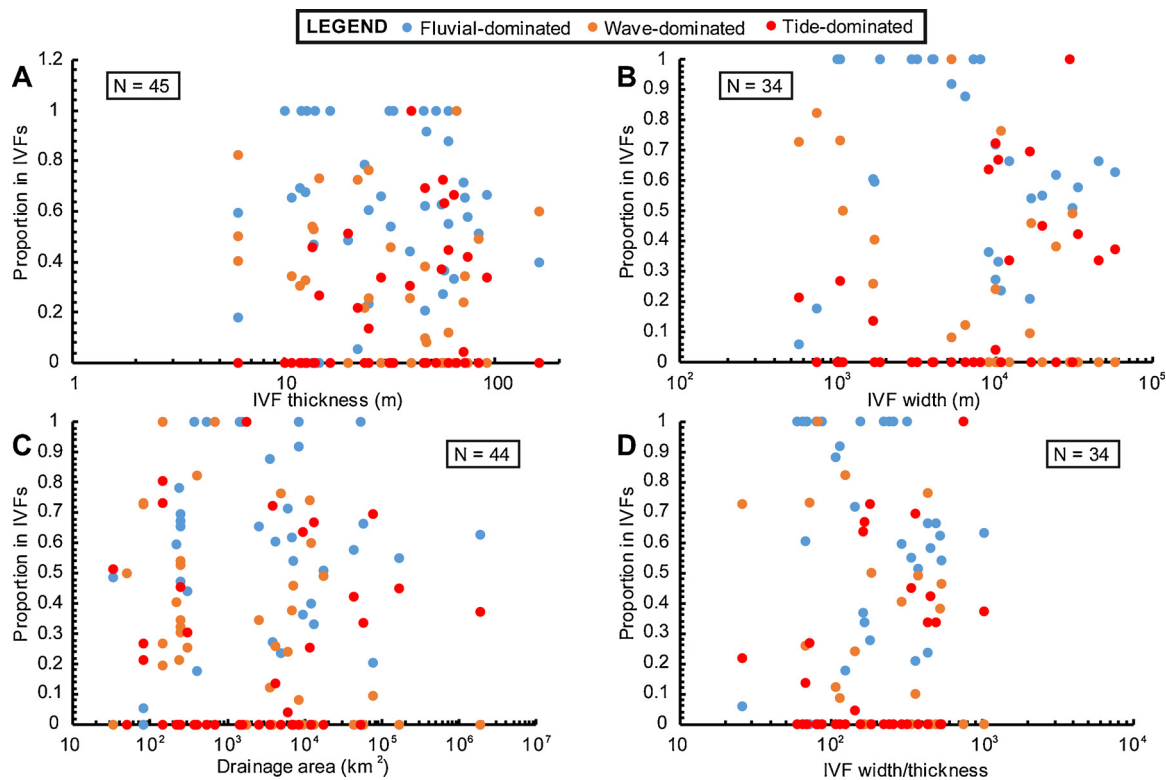


Fig. 10. Cross-plots of proportion of architectural elements (Scheme 2) within coastal-plain incised-valley fills versus IVF thickness (A), width (B), drainage-basin area (C) and width-to-thickness ratio (D). Architectural elements are classified on their dominant process regime. For each pair of variables, the correlation coefficients and P-values are reported in respective cell in Table 5. 'N' denotes the number of incised-valley fills.

4.2. Controls on the internal fills of incised valleys

4.2.1. Continental-margin type

Incised-valley systems are likely to record variations in sediment yield, sediment supply, and resulting shoreline progradation rates and rates at which drowned-valley estuaries undergo continentalization

(Dalrymple, 2006; Wilson et al., 2007; Clement et al., 2017; Clement and Fuller, 2018), which themselves might be expected to vary characteristically across types of continental margins. The results presented in this study (Fig. 7A) indicate that a higher proportion of fluvial deposits and a lower proportion of central-basin estuarine deposits are observed in incised-valley fills hosted on active margins compared to

Table 5

Correlation coefficients and P-values reported for the relationship between the proportion of fluvial-dominated, wave-dominated and tide-dominated elements within IVFs versus IVF thickness, IVF width and drainage area. 'N' denotes the number of readings, 'R' denotes Pearson's R, and 'r' denotes Spearman's rho.

Elements	IVF thickness	IVF width	Drainage area	IVF width/thickness
Fluvial-dominated	N = 45; R = -0.081, p = 0.596; r = -0.085, p = 0.58	N = 34; R = -0.146, p = 0.412; r = -0.161, p = 0.362	N = 44; R = 0.062, p = 0.690; r = 0.178, p = 0.247	N = 34; R = -0.165, p = 0.350; r = -0.179, p = 0.310
Wave-dominated	N = 45; R = -0.056, p = 0.715; r = -0.201, p = 0.185	N = 34; R = -0.217, p = 0.218; r = -0.246, p = 0.161	N = 44; R = -0.176, p = 0.252; r = -0.337, p = 0.025	N = 34; R = -0.153, p = 0.389; r = -0.111, p = 0.530
Tide-dominated	N = 45; R = 0.160, p = 0.294; r = 0.293, p = 0.051	N = 34; R = 0.414, p = 0.015; r = 0.457, p = 0.007	N = 44; R = 0.112, p = 0.469; r = 0.129, p = 0.403	N = 34; R = 0.369, p = 0.032; r = 0.271, p = 0.120

those on passive margins. These observations contrast with the fact that passive margins are typically associated with larger rivers (Syvitski and Milliman, 2007; Sømme et al., 2009a), and are therefore usually associated with (i) higher rates of sediment supply (Syvitski and Milliman, 2007; Blum et al., 2013), which control shoreline progradation rates, and (ii) with larger maximum bankfull depths, which translate to thicker channel belts, bars and channel fills (Fielding and Crane, 1987; Bridge and Mackey, 1993; Shanley, 2004; Fielding et al., 2006; Gibling, 2006; Blum et al., 2013). An explanation of this inconsistency appears elusive. The lower proportion of central-basin deposits within incised-valley fills along active margins could be explained by the nature of sediment load carried by the respective river systems. River systems along passive margins are generally larger than their active-margin counterparts, and tend to carry high suspended-sediment load, which can feed estuaries and be deposited as fluid muds around the turbidity maximum (e.g., Portela et al., 2013; Carlin et al., 2015).

Previous work (Wang et al., 2019) has demonstrated that incised-

valley fills along active margins tend to be thicker and wider on average than those along passive margins. This may be seen because active margins are generally associated with higher-gradient shelves, resulting in larger differences between the shelf gradient and the lowstand fluvial equilibrium profile, which in turn favours deeper fluvial incision for a given sea-level fall (Schumm and Brackenkridge, 1987; Leckie, 1994; Posamentier and Allen, 1999). Moreover, active margins are generally associated with high specific sediment yield and rivers that drain active margins tend to have a high bedload-to-suspended-load ratio (Milliman and Syvitski, 1992), which promotes more rapid attainment of equilibrium profiles (Dietrich and Whiting, 1989; Sheets et al., 2002; Peakall et al., 2007; Martin et al., 2011; Blum et al., 2013); a tendency to reach equilibrium more easily might therefore result in fluvial incision being deeper, on average, than what is typical for passive-margin valleys. The observation that estuarine bay/lagoon elements are thicker on average in incised-valley fills along active margins than in those along passive margins (Fig. 7B) might arise because valleys along active margins, by

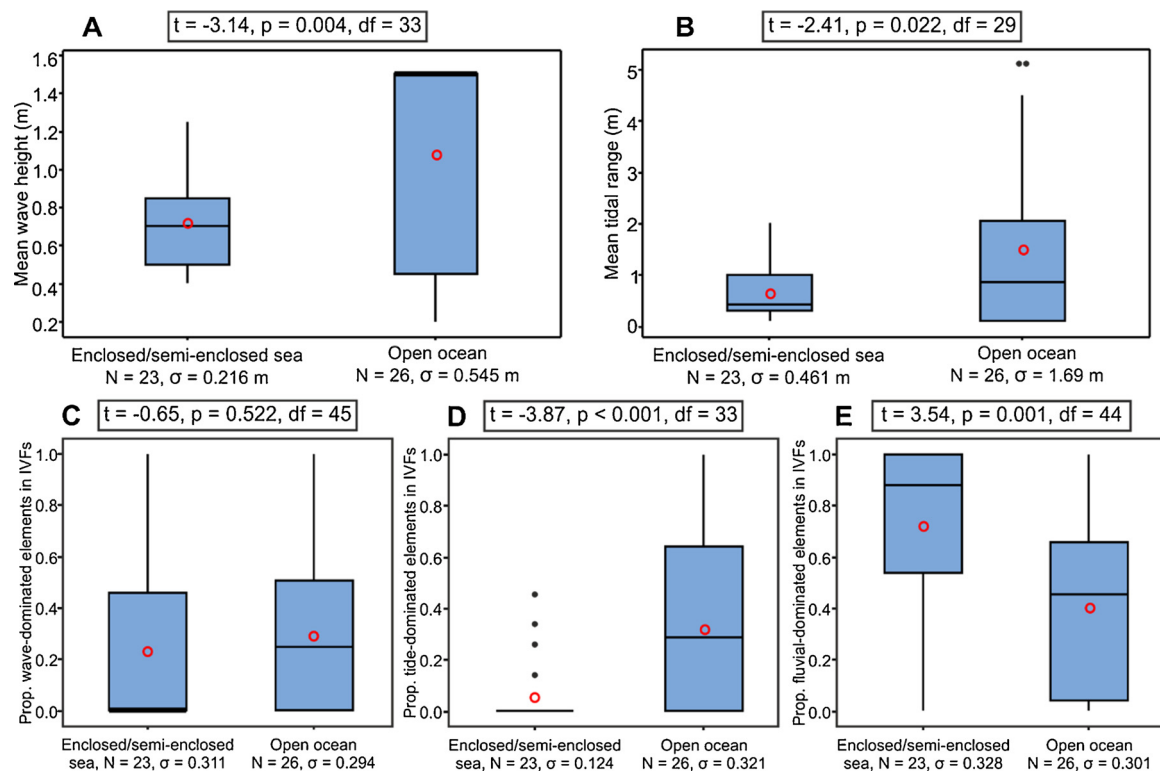


Fig. 11. (A, B) Box-plots of distributions of mean wave height (A) and mean tidal range (B) at the present-day shoreline of the studied coastal-plain incised-valley fills associated with enclosed or semi-enclosed seas and with open oceans. (C–E) Box-plots of distributions of the proportion of architectural elements (Scheme 2; see Table 2) in coastal-plain IVFs for enclosed/semi-enclosed seas and open oceans. For each box-plot, boxes represent interquartile ranges, red open circles represent mean values, horizontal bars within the boxes represent median values, and black dots represent outliers (values that are more than 1.5 times the interquartile range). 'N' denotes the number of readings. ' σ ' denotes the standard deviation. The results of two-sample t-test (t-value, P-value and degrees of freedom) are reported in boxes.

Table 6

Correlation coefficients and P-values reported for the relationship between mean wave height, mean tidal range at present-day shorelines and the proportion of fluvial-dominated, wave-dominated and tide-dominated elements within coastal-plain IVFs versus shelf width, shelf-break depth and shelf gradient (N = 49). 'N' denotes the number of incised-valley fills, 'R' denotes Pearson's R, and 'r' denotes Spearman's rho.

Quantity	Shelf width	Shelf-break depth	Shelf gradient
Mean wave height	R = 0.093, p = 0.547; r = 0.171, p = 0.267	R = 0.496, p < 0.001; r = 0.430, p = 0.002	R = 0.200, p = 0.168; r = 0.260, p = 0.071
Mean tidal range	R = 0.077, p = 0.617; r = -0.109, p = 0.481	R = 0.260, p = 0.071; r = -0.027, p = 0.853	R = -0.228, p = 0.115; r = -0.233, p = 0.108
Proportion of fluvial-dominated deposits	R = 0.204, p = 0.183; r = 0.176, p = 0.252	R = -0.230, p = 0.111; r = -0.229, p = 0.114	R = -0.140, p = 0.336; r = -0.239, p = 0.097
Proportion of wave-dominated deposits	R = -0.174, p = 0.258; r = -0.099, p = 0.523	R = 0.100, p = 0.493; r = 0.191, p = 0.190	R = 0.346, p = 0.015; r = 0.449, p = 0.001
Proportion of tide-dominated deposits	R = -0.080, p = 0.607; r = -0.024, p = 0.878	R = 0.181, p = 0.214; r = 0.247, p = 0.087	R = -0.195, p = 0.180; r = -0.155, p = 0.288

being more deeply incised on average, will also tend to host greater accommodation. This might favour the development of thicker estuarine bay/lagoon elements within valley fills on active margins. The results suggest that continental margin types exert an indirect effect on the geometry of estuarine bay/lagoon element within incised-valley fills through a control on valley morphology.

Results from this study suggest that the type of continental margin might be taken as a predictor of the internal fills of incised valleys, likely because of the effects of the tectonic setting on basin physiography, rates and mode of sediment supply, and nature of sediment load. This view is in part supported by the result of principal component analysis (see Supplementary information; text and Fig. S1A) applied to a limited dataset of 30 IVFs for which eight variables can be constrained; this analysis indicates that overall the studied IVFs tend to display differences in the studied variables that map onto the type of continental margin on which they are hosted.

4.2.2. Shelf physiography

The development of barrier islands that can be stranded on the shelf during TST tend to develop in association with stadials during deglaciation, i.e., in relation with periods of negligible or slow rates of relative sea-level rise known as stillstands or slowstands (e.g., Cooper, 1958, 1991; Trincardi et al., 1994; Storms et al., 2008; Salzmann et al., 2013). Preservation of these barrier islands on the shelf during transgression is believed to be facilitated by factors such as rapid sea-level rise after stillstands (e.g., Storms et al., 2008; Salzmann et al., 2013), early cementation of the barrier form (Gardner et al., 2005, 2007; Salzmann et al., 2013; Green et al., 2013a, 2014), and gentle antecedent shelf gradient and reduced wave-energy (Cooper et al., 2016;

Storms et al., 2008). Rapid sea-level rise after stillstands is shown to be conducive to the preservation of barrier-island deposits (Belknap and Kraft, 1981; Forbes et al., 1995; Storms et al., 2008; Salzmann et al., 2013). Rapid sea-level rise is typically associated with only limited reworking or breakdown of the barrier form during ensuing transgressive ravinement (Storms et al., 2008; Salzmann et al., 2013; Cooper et al., 2016). Antecedent shelf gradient is also shown to be a control on the preservation of barrier islands (Storms et al., 2008; Salzmann et al., 2013; Pretorius et al., 2016; Green et al., 2018). Cattaneo and Steel (2003) point out that, given the same unit of time of relative sea-level rise, the effects of erosion at the shoreline across high-gradient shelves is much greater than that across low-gradient shelves during ensuing transgressive ravinement, resulting in severe reworking or breakdown of the barrier systems. This is because the shoreline does not translate over a large distance for the same amount of sea-level rise and erosion is therefore focussed over a shorter profile for the same unit of time (Davis and Clifton, 1987). However, the results of this study (Fig. 12) challenge the applicability of this notion to incised-valley systems, as positive correlations are observed between the thickness and proportion of barrier-complex deposits within incised-valley fills versus the average shelf gradient in the last sea-level cycle. Previous work documents that equilibrium in sandy shorelines is attained over timescales of 10^2 to 10^3 years (Cowell and Thom, 1994; Stive and de Vriend, 1995). For a given relative sea-level change, horizontal shoreline shifts increase in magnitude with decreasing shelf gradient. Thus, compared to lower-gradient shelves, any high-energy environment located in the area of the coastline across steeper-gradient shelves will stabilize at a location for longer periods during episodes of negligible or slow rates of relative sea-level rise, potentially promoting accumulation of barrier-complex

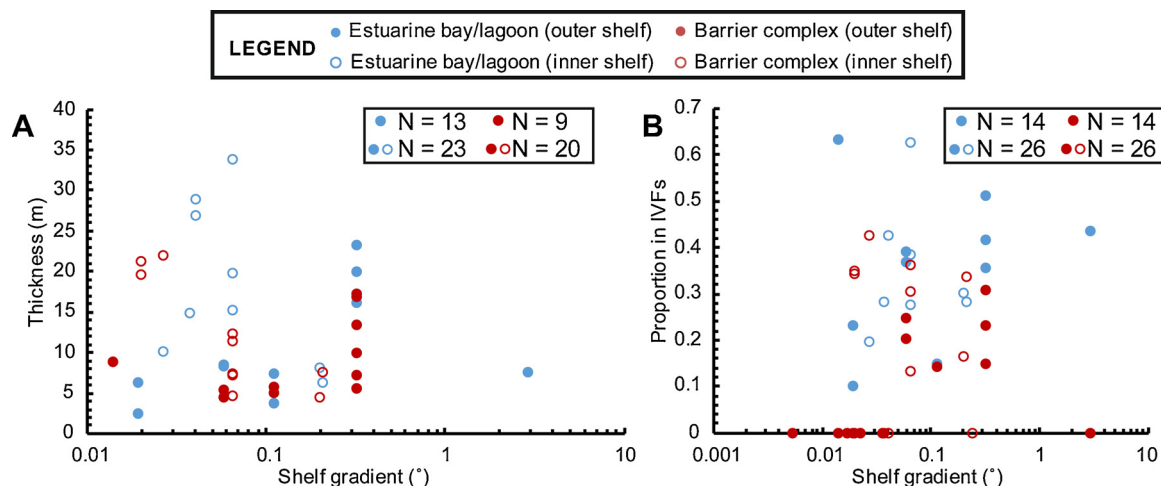


Fig. 12. Plots of thickness (A) and proportion (B) of architectural elements within cross-shelf incised-valley fills versus shelf gradient. For each pair of variables, the correlation coefficients and P-values are reported in respective cell in Table 7. 'N' denotes the number of readings.

Table 7

Correlation coefficients and P-values reported for the relationship between the thickness or proportion of estuarine bay/lagoon and barrier complex elements within IVFs versus shelf gradient. Note that these two elements are classified into two groups, i.e., those hosted on the outer shelf and those hosted on the inner shelf. 'N' denotes the number of readings, 'R' denotes Pearson's R, and 'r' denotes Spearman's rho.

Parameters	Elements	Position	Shelf gradient
Thickness	Estuarine bay/lagoon	Outer shelf	N = 13; R = -0.004, p = 0.990; r = 0.531, p = 0.062
		Shelf	N = 23; R = -0.139, p = 0.538; r = 0.122, p = 0.588
	Barrier complex	Outer shelf	N = 9; R = 0.546, p = 0.128; r = 0.741, p = 0.022
		Shelf	N = 20; R = -0.232, p = 0.340; r = -0.226, p = 0.351
Proportion	Estuarine bay/lagoon	Outer shelf	N = 14; R = 0.314, p = 0.274; r = 0.494, p = 0.072
		Shelf	N = 26; R = 0.245, p = 0.228; r = 0.49, p = 0.011
	Barrier complex	Outer shelf	N = 14; R = -0.107, p = 0.715; r = 0.625, p = 0.017
		Shelf	N = 26; R = -0.142, p = 0.487; r = 0.325, p = 0.106

deposits within cross-shelf valleys (e.g., Posamentier, 2001; Reijenstein et al., 2011; Wetzel et al., 2017). The control by shelf gradient on transgression also plays an indirect role on the erodibility of barrier deposits when accompanied with climate. It has been proposed (Frankel, 1968; Hopley, 1986; Moore, 2001; Voudoukas et al., 2007; Cawthra and Uken, 2012) that the rates of shoreline cementation in warm tropical or sub-tropical climates can be particularly rapid, occurring on a scale of months to decades. Hence, longer periods of early cementation of the barriers along steeper shelves, prior to barrier overstepping, might make the barrier deposits more resistant to erosion during ensuing transgressive ravinement. Positive correlations between both the thickness and proportion of barrier-complex elements versus the average shelf gradient (Fig. 12) support the idea that the shelf gradient plays a role in controlling the establishment and preservation of barrier-complex deposits within incised valleys hosted on the shelf. However, these observations are based on limited data (N = 9 for the thickness of barrier-complex elements and N = 14 for the proportion of barrier-complex elements) and thus any conjecture on the effective role of shelf gradient on the development and preservation of barrier-complex deposits within valley fills needs to be substantiated through further study. Additionally, expected relationship between shelf gradient and characteristics of barrier-complex deposits in incised-valley fills might be masked by overriding factors, such as early cementation controlled by palaeo-climates, or wave and tide energy regimes, or by the fact that the present-day average shelf gradient does not approximate the local shelf gradient established during transgression.

Positive correlations between the proportion of estuarine bay/lagoon elements versus the average shelf gradient (Fig. 12B) are attributed to the fact that steeper shelves could result in larger difference between shelf gradient and the fluvial equilibrium profile and therefore should tend to drive deeper fluvial incision for a given relative sea-level fall (Schumm and Brackenridge, 1987; Leckie, 1994; Posamentier and Allen, 1999; Wang et al., 2019), thereby providing increased accommodation for estuarine bay/lagoon deposits that can be preserved in incised valleys. Thus, the shelf gradient may exert an indirect control on the development and preservation of the geometry of estuarine bay/lagoon deposits within cross-shelf incised valleys through its effects on incised-valley dimensions and the resultant accommodation space.

4.2.3. Catchment and river-system size

Positive correlations between the thickness or proportion of LST deposits versus incised-valley-fill dimensions (Fig. 8) might reflect how these parameters tend to co-vary in relation to a common control exerted by the size of drainage areas. Previous work (Mattheus et al., 2007; Mattheus and Rodriguez, 2011; Phillips, 2011; Wang et al., 2019) has demonstrated that the size of incised valleys shows positive correlation with the size of their drainage basins. Water discharge, which is positively correlated with drainage-basin area (Syvitski and Milliman, 2007), controls the maximum bankfull depth of a river. Hence, river size and the geometry of fluvial deposits (thickness of barforms, channel fills and channel belts) are expected to be scaled to drainage-

basin area. Positive scaling relationships between drainage-basin area, water discharge, single-storey channel-belt sand-body thickness (channel-fill or barform thickness), and river size are recognised in studies based on late-Quaternary examples (Blum et al., 2013), compilation of ancient channel-belt scales from published literature (Gibling, 2006) and regional case studies (e.g., Shanley, 2004; Fielding et al., 2006). Thus, these results might reflect the fact that the development of valleys having larger drainage basins and characterized by higher bankfull discharges will tend to be filled by thicker fluvial deposits preserved in LSTs. It needs to be considered, however, that relationships between the thickness and proportion (thickness ratio) of LST deposits in incised-valley fills and the size of the valley catchments – albeit positive – are modest and not statistically significant (Table 3).

Sedimentation associated with the TST takes place when accommodation is being created at its fastest rate by relative sea-level rise. Positive correlation between the thickness of TST deposits versus incised-valley-fill thickness (Fig. 8A) can be explained by the fact that deeper valleys will be more likely to record the full expression of a TST and to contain maximum flooding surfaces within their confines. However, this interpretation is at odd with the fact that no significant difference exists between the thickness distributions for incised-valley fills that contain HST deposits compared to those that were overfilled and/or ravined during transgressions and do not contain HST deposits.

Positive correlations between the thickness of fluvial deposits versus incised-valley-fill dimensions (Fig. 9A–C) might reflect how these variables are expected to co-vary in relation to a common control exerted by the size of drainage areas. The results suggest that the thickness of fluvial deposits in valley fills might reflect the thickness of channel belts, which is itself controlled by the size of their drainage-basin areas.

Based on studies of the internal fills of modern estuaries in New Zealand (e.g., Heap and Nichol, 1997; Wilson et al., 2007; Abraham et al., 2008; Kennedy et al., 2008; Clement et al., 2017), it has been proposed that shallower estuaries are more easily backfilled than deeper ones, especially when they are coupled with river systems with high sediment supply, such that the relatively restricted space within valley fills tends to limit the development of deeper central-basin environments (estuarine bay/lagoon deposits), where fine-grained sediments accumulate. Additionally, large river systems associated with low-gradient coastal plains – typical of passive margins – are prone to carrying substantial suspended-sediment load when they reach the sea (Milliman and Syvitski, 1992). These fine-grained sediments can feed estuaries and be deposited as fluid muds around the turbidity maximum (e.g., Portela et al., 2013; Carlin et al., 2015), especially if tidal processes are important (e.g., Dalrymple et al., 2012). Positive relations between the thickness of estuarine bay/lagoon elements versus incised-valley-fill dimensions and drainage-basin area (Fig. 9A–C) support these expectations only to a certain degree, as the thickness of the valley may not necessarily be a good proxy for the depth of the estuary during TST or HST. The results suggest that both drainage-basin area and incised-valley geometry could act as factors that control the

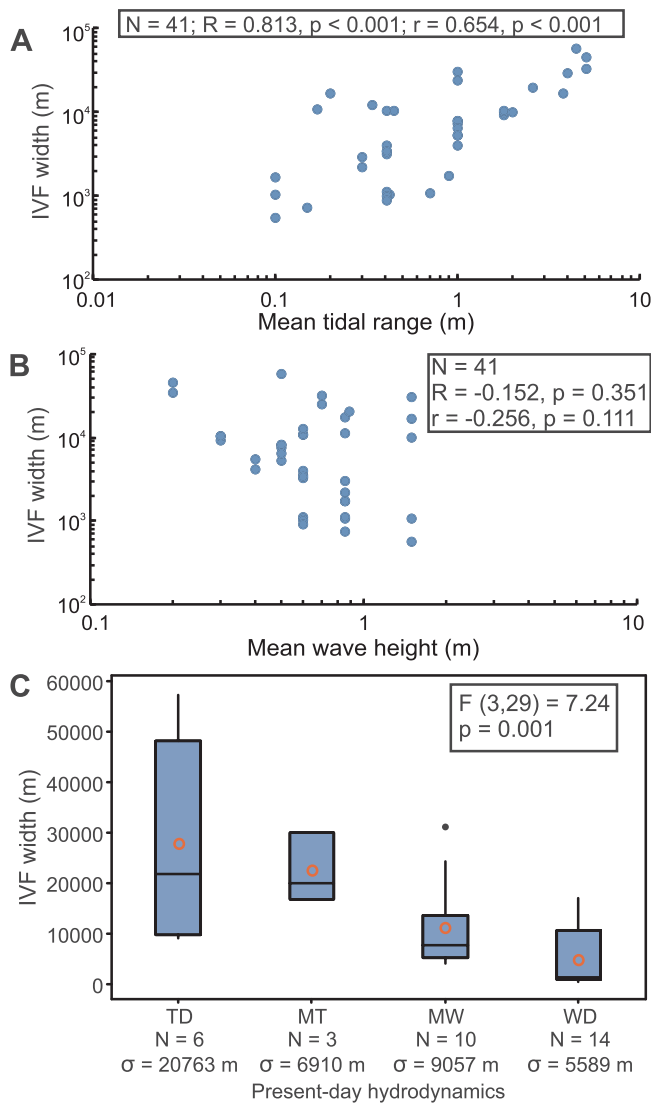


Fig. 13. Individual-value plot of thickness ratios of HSTs in coastal-plain valley fills (A) and of the proportion of architectural elements (Scheme 2; F: fluvial-dominated deposits; T: tide-dominated deposits; W: wave-dominated deposits) in the HST of coastal-plain incised-valley fills (B) for different hydrodynamic regimes at modern shorelines (TD: tide dominated; MT: mixed tide dominated; MW: mixed wave dominated; WD: wave dominated). For each pair of variables, the correlation coefficients and P-values are reported in respective boxes. 'N' denotes the number of readings, 'R' denotes Pearson's R, and 'r' denotes Spearman's rho. (C) Box plot of distributions of incised-valley-fill width for different present-day hydrodynamic regimes (TD: tide dominated; MT: mixed tide dominated; MW: mixed wave dominated; WD: wave dominated). For each box plot, boxes represent interquartile ranges, red open circles represent mean values, horizontal bars within the boxes represent median values, and black dots represent outliers (values that are more than 1.5 times the interquartile range). 'N' denotes the number of readings. 'σ' denotes the standard deviation. The results of one-way ANOVA are reported in the box in part C, as: F-value (degrees of freedom between and within groups in brackets), P-value.

accumulation of estuarine deposits preserved within incised valleys.

Positive correlations between the thickness of bayhead-delta deposits versus drainage-basin area (Fig. 9C) could possibly reflect the fact that more rapidly prograding bayhead deltas associated with larger river systems will have advanced into deeper parts of their estuaries. However, this interpretation carries significant uncertainty as the 3D geometry of bayhead delta deposits is not typically characterized, and packages of bayhead-delta deposits may incorporate vertically amalgamated lobes that cannot be resolved in core.

Overall, the size of drainage areas appears to control the thickness

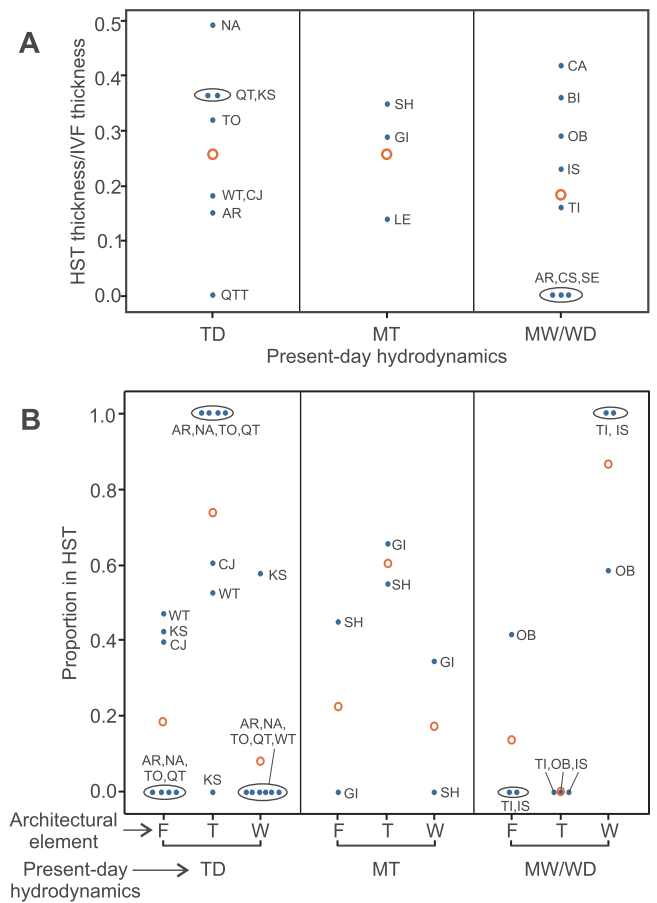


Fig. 14. (A, B) Cross-plots of incised-valley-fill width versus mean tidal range (A) and mean wave height (B) at the modern shoreline. For each pair of variables, the correlation coefficients and P-values are reported in respective boxes. 'N' denotes the number of readings, 'R' denotes Pearson's R, and 'r' denotes Spearman's rho. (C) Box plot of distributions of incised-valley-fill width for different present-day hydrodynamic regimes (TD: tide dominated; MT: mixed tide dominated; MW: mixed wave dominated; WD: wave dominated). For each box plot, boxes represent interquartile ranges, red open circles represent mean values, horizontal bars within the boxes represent median values, and black dots represent outliers (values that are more than 1.5 times the interquartile range). 'N' denotes the number of readings. 'σ' denotes the standard deviation. The results of one-way ANOVA are reported in the box in part C, as: F-value (degrees of freedom between and within groups in brackets), P-value.

of fluvial deposits, of bayhead-delta deposits and of estuarine bay/lagoon deposits in incised-valley fills (Fig. 9A to C) through its effects on water discharge, sediment supply, the character of sediment load and in-valley accommodation related to incised-valley geometry.

4.2.4. Shoreline hydrodynamics

4.2.4.1. Control of hydrodynamic conditions on sedimentation. Hydrodynamic conditions at the shoreline control the deposition and preservation potential of sedimentary bodies in estuaries (Tessier et al., 2010a, 2010b; Menier et al., 2010; Proust et al., 2010; Ferrer et al., 2010; Tessier, 2012). Wave-dominated estuaries are typically characterized by a barrier beach and a tidal-inlet complex at their mouth, passing landward into central-basin muds and bayhead delta deposits (Dalrymple et al., 1992; Dalrymple and Zaitlin, 1994; Ferrer et al., 2010; Tesson et al., 2010). Tide-dominated estuaries are typically characterized by tidal sandbars that grade to mudflats and salt marshes up-estuary (Dalrymple et al., 1992; Dalrymple and Zaitlin, 1994; Tessier, 2012). In highstand deposits, the observation of higher proportions of tide-dominated elements (e.g., tidal flat and tidal channel, tidal sand-bar complex, tidal inlet and flood tidal delta

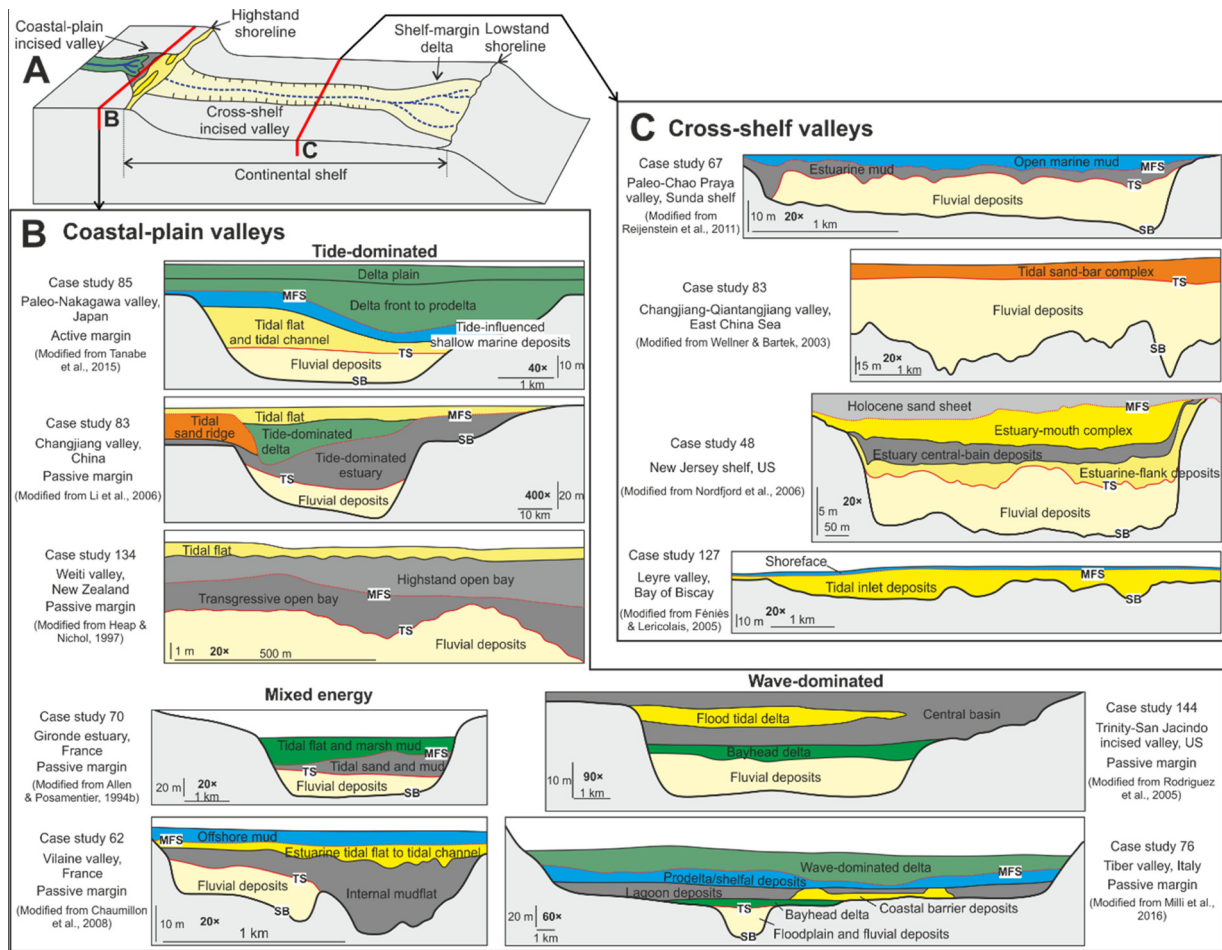


Fig. 15. Example stratigraphic architectures of incised-valley fills, illustrating the variability observed along strike-oriented cross sections for some of the late-Quaternary coastal-plain (B) and cross-shelf (C) valley fills considered in this work. In (B), the examples for coastal-plain valley fills are grouped by classes of present-day hydrodynamic regimes at the shoreline; continental-margin types are also indicated. Key sequence-stratigraphic bounding surfaces (SB, TS and MFS) are shown for examples for which sequence-stratigraphic interpretations were presented in the original source work. SB denotes the sequence boundary, TS denotes the transgressive surface, and MFS denotes the maximum flooding surface.

subenvironment) in valley fills associated with full or mixed-energy tide-dominated conditions than in those with more wave-dominated conditions (Fig. 13B) indicates the expected increased dominance of tidal processes on sedimentation. Likewise, higher proportions of wave-dominated elements (e.g., nearshore, barrier complex subenvironments) in valley fills associated with full to mixed-energy wave-dominated conditions than in those with more tide-dominated conditions (Fig. 13B) indicate the expected increased dominance of wave processes on sedimentation. The results (Fig. 13B) likely reflect the importance of hydrodynamic processes in determining the types of sub-environments recorded as sedimentary bodies in the HST of coastal-plain incised-valley fills.

Based on the synthesis of data from 10 incised valleys that occur along the Mediterranean and Atlantic coasts of France, Chaumillon et al. (2010) argued that within the outer segments of the valley fills (cross-shelf valley fills, in this paper), the HST to TST ratio increases from wave-dominated to tide-dominated settings because of the deeper wave base offshore wave-dominated coasts. Chaumillon et al. (2010) also proposed that in the middle segments of the valley fills (coastal-plain valley fills, in this paper), the thickness of HSTs does not vary significantly across different hydrodynamic regimes, despite differences seen in the types of sub-environments incorporated in the HST of valley fills under different hydrodynamic conditions. Our data (Fig. 13A) support the claim made by Chaumillon et al. (2010) for coastal-plain valley fills, but any interpretation is highly uncertain, as the dataset is

limited ($N = 19$).

4.2.4.2. Control of hydrodynamic conditions on IVF geometry. With regards to the relationship between incised-valley-fill width and present-day hydrodynamic regimes, Mattheus and Rodriguez (2011) argued that bay-ravinement, or estuarine shoreline erosion, which is controlled by the imposing energy regime of waves and tides, can lead to the widening of incised valleys. However, our data (Fig. 14) do not fully support this idea, as no apparent correlation is seen between incised-valley-fill width versus mean wave height at modern shorelines. This might arise because wave ravinement tends to truncate the topmost part of the interfluvial of some incised valleys, where each valley is expected to have been widest (Fig. 16A); this fact might counteract the effects of any widening of the incised valleys by wave erosion. This discrepancy might also arise from the fact that the present-day hydrodynamic conditions at the shoreline may not be representative of those that existed during the late TST or due to the influence of other factors such as catchment size, vegetation, substrate and climate.

Positive correlation between incised-valley-fill width versus present-day mean tidal range at the shoreline (Fig. 14A) could be explained by the fact that tidal ravinement might drive erosion of valley margins, which promotes the widening of the incised valleys (Fig. 16B).

4.2.4.3. Control of IVF geometry on hydrodynamic conditions. The

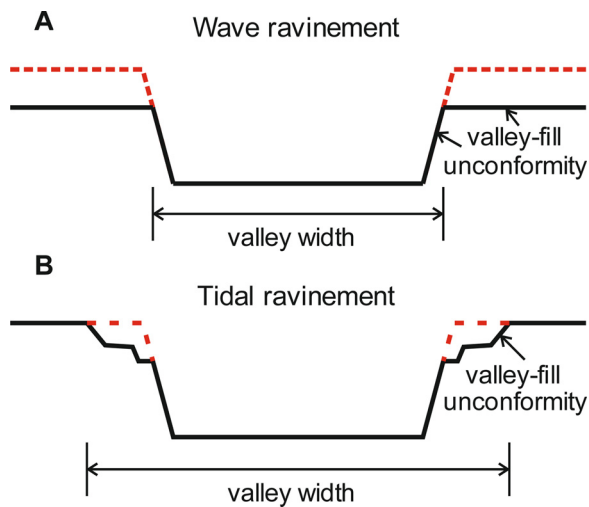


Fig. 16. Schematic diagrams illustrating the evolution of valley width in response to wave ravinement (A) and tidal ravinement (B). Red dashed line denotes the pre-ravinement valley shape.

geometry of incised valleys being flooded has also been recognized as a factor controlling the internal fills of incised valleys through its control on hydrodynamic conditions (Dalrymple et al., 1992; Chaumillon et al., 2010; Nordfjord et al., 2006). The tidal prism at any location is a function of the shape of the drowned-valley estuaries, their geographic orientation, shelf geometry, tidal resonance, which itself is determined by shelf width and shelf depth, and frictional forces (Luketina, 1998; Hume, 2005; Davis et al., 2009). Generally, funnel-shaped valleys tend to enhance the amplification of tidal waves and thus the occurrence of tide-dominated conditions (Dalrymple et al., 1992; Chaumillon et al., 2010; Tessier et al., 2012). Based on observations of seismic data of late-Quaternary incised-valley fills on the New Jersey shelf, Nordfjord et al. (2006) argued that narrower and deeper valleys should promote the development of tide-dominated environments, whereas broader valleys might be, comparatively, more dominated by wave processes. However, our observations (Fig. 10) do not support the assumption made by Nordfjord et al. (2006). Positive correlation between incised-valley-fill width and the proportion of tide-dominated elements (Fig. 10B) might reflect how these two variables co-vary in response to a common control exerted by the present-day hydrodynamic regime (mean tidal range) at the shoreline (Figs. 13B and 14 A). This observation (Fig. 10B) could also be explained by the fact that wider valleys with gentler gradient, generally associated with larger rivers, will tend to have larger tidal prism and thus experience stronger tidal currents. Furthermore, for narrow and linear valleys, tidal flow tends to be dampened by friction on the valley margins and tidal-wave energy is dissipated by diffraction. Thus, our observations (Fig. 10B) can be seen to support the idea that the influence of valley geometry on tides leaves a distinct sedimentary record; else, they reflect the control of present-day mean tidal range at the shoreline on incised-valley-fill width. However, this interpretation carries uncertainty, as the present-day incised-valley-fill geometry is in part used as a proxy for the valley geometry through time, ignoring temporal variations in valley geometry (cf. Blum and Price, 1998; Rodriguez et al., 2008; Blum et al., 2013).

No or weak correlations are seen between the proportion of wave-dominated elements in IVFs and parameters that describe the IVF geometry. However, detailed descriptors of the planform shape of the valley and of the morphology of the bedrock, which might affect the extent to which an IVF could be exposed to wave action, were not considered in this work.

4.2.4.4. Control of basin physiography on hydrodynamic conditions. Other

authors (Healy and Werner, 1987; Healy and Harada, 1991b) have proposed that, compared to open-ocean-facing settings, the coasts of enclosed or semi-enclosed seas generally experience lower hydrodynamic energy. This is especially true for coasts characterized by offshore topographic sills that can shelter the shorelines. Enclosed or semi-enclosed seas are generally characterized by more restricted fetch, lower wave heights, and lower tidal range. Our observations (Fig. 11) are compatible with the idea that the type of coastal physiography and size of the sea into which a valley discharges could act as controls on the internal fills of coastal-plain incised valleys, since variations in the record of dominant depositional processes are seen in the valley fills that are consistent with differences in hydrodynamic conditions across these settings.

Wave energy at the shoreline depends largely on deep-water wave energy, the water depth of the basin and the frictional attenuation that occurs on the shelf (Reading and Collinson, 1996). This frictional attenuation is determined by the gradient of the sea floor, which itself is a function of the nature and width of the shelf and the rate and type of sediment supply to the nearshore zone. Positive correlations between mean wave height and shelf-break depth and between the proportion of wave-dominated elements in IVFs and the average shelf gradient (Table 6) could be explained by the fact that the shorelines of shallower shelves tend to be subject to lower wave energy.

5. Conclusions

A database-driven statistical analysis of 87 late-Quaternary incised-valley fills has been undertaken, to assess the general validity of classical facies models that remain widely employed as predictive tools, and investigate the relative importance of different controls on the stratigraphic organization of incised-valley fills. The main findings are summarized as follows.

- 1 The general stratigraphic organization of the studied coastal-plain incised-valley fills is consistent with what represented in classical facies models, but significant variability in stratigraphic architectures is seen.
- 2 Compared to the studied coastal-plain valleys, the internal fills of valleys incised into modern shelves are characterized by a higher proportion of lowstand deposits and a higher proportion of open-shelf sediments.
- 3 Compared to valley fills hosted on passive margins, a higher proportion of fluvial deposits, a lower proportion of central-basin estuarine deposits and thicker central-basin estuarine deposits are typically observed in incised-valley fills hosted on active margins; this is interpreted as reflecting a control by the tectonic setting of continental margins on the internal fills of incised valleys, through its effects on basin physiography, rates and mode of sediment supply, and nature of sediment load.
- 4 The thickness or proportion of LST deposits is found to be positively correlated with incised-valley-fill dimensions, likely because of the role of the size of catchment areas and water discharge in dictating the scale of lowstand fluvial systems.
- 5 Positive scaling shown by the thickness of fluvial, bayhead-delta, and estuarine bay/lagoon with incised-valley-fill dimensions and valley drainage-basin area suggests that the valley catchment size controls the scale of these deposits, possibly through effects on water discharge, sediment supply, sediment-load type, and incised-valley geometry.
- 6 Positive correlations between the thickness and proportion of barrier-complex deposits within incised-valley fills versus present-day average shelf gradient indicate a possible control by the physiography of the shelf on the establishment and preservation of barrier-island environments within incised valleys.
- 7 The gradient of the shelf may also exert an indirect control on the development and preservation of the geometry of estuarine muds in

cross-shelf valley fills by partly determining depths of incisions and resultant in-valley accommodation.

- Correlations between incised-valley-fill width versus present-day mean tidal range or mean wave height at the shoreline indicate that tidal dynamics at the shoreline may control the widening of the incised valleys. Correlation between the proportion of tide-dominated elements within incised-valley fills and incised-valley-fill width might arise because of reciprocal controls between hydrodynamic conditions and valley geometry.
- Differences in proportion of elements recording different process regimes are seen between valley fills from open-ocean settings and those from enclosed or semi-enclosed seas, which are consistent with differences in hydrodynamic conditions across these settings.

This study is important because it highlights the complexity of the internal sedimentary fills of incised valleys to a level of detail that is not accounted for by the general stratigraphic organization depicted by widely employed traditional facies and sequence-stratigraphic models. This work highlights the role of continental-margin type, drainage-basin area, valley geometry, basin physiography and shoreline hydrodynamics – in addition to the role of relative sea-level stage – in controlling the internal architecture of incised valley fills.

These results can be applied to guide interpretations and attempt predictions of the architecture of ancient paralic successions, in the subsurface and in outcrop. However, all the studied examples are from the late Quaternary, and record relatively high-frequency, high-amplitude changes in sea level: care must therefore be taken when attempting to use these examples as templates for interpreting or predicting the stratigraphic architecture of ancient systems, especially for those developed under greenhouse climates and subject to modest sea-level fluctuations.

Acknowledgements

Ru Wang has been supported by a scholarship from China Scholarship Council associated with University of Leeds (Grant number 201606440059). FRG-ERG and SMRG sponsors and partners AkerBP, Anadarko, Areva (now Orano), BHPBilliton, Cairn India (Vedanta), ConocoPhillips, Chevron, Debmarine, Engie, Murphy Oil, Nexen-CNOOC, Petrotechnical Data Systems, Saudi Aramco, Shell, Tullow Oil, Woodside and YPF are thanked for their financial support of the research. Luca Colombera has been supported by NERC (Catalyst Fund award NE/M007324/1; Follow-on Fund NE/N017218/1). Ru thanks for the spiritual support from her parents and good friends Xueting Wu, Yinzhi Wang, Xin Zhao, Xiangru Shi and Peng Huang. We thank four anonymous reviewers and Editor Chris Fielding for their comments, which have improved this article.

Appendix A. Supplementary data

Supplementary material related to this article can be found, in the online version, at doi:<https://doi.org/10.1016/j.earscirev.2019.102988>.

References

- Abraham, G.M., Nichol, S.L., Parker, R.J., Gregory, M.R., 2008. Facies depositional setting, mineral maturity and sequence stratigraphy of a Holocene drowned valley, Tamaki Estuary, New Zealand. *Estuarine, Coastal and Shelf Science* 79, 133–142.
- Allard, J., Chaumillon, E., Féliens, H., 2009. A synthesis of morphological evolutions and Holocene stratigraphy of a wave-dominated estuary: the Arcachon lagoon, SW France. *Cont. Shelf Res.* 29, 957–969.
- Allen, G.P., Posamentier, H.W., 1993. Sequence stratigraphy and facies model of an incised valley fill; the Gironde Estuary, France. *J. Sediment. Res.* 63, 378–391.
- Allen, G.P., Posamentier, H.W., 1994a. Sequence stratigraphy and facies model of an incised valley fill: the Gironde Estuary, France: reply. *J. Sediment. Res.* B64, 81–84.
- Allen, G.P., Posamentier, H.W., 1994b. Transgressive facies and sequence architecture in mixed tide-and wave-dominated incised valleys: example from the Gironde Estuary, France. In: Dalrymple, R.W., Boyd, R., Zaitlin, B.A. (Eds.), *Incised-Valley Systems: Origin and Sedimentary Sequences* 51. SEPM Special Publications, pp. 225–239.
- Allen, G.P., 1991. Sedimentary processes and facies in the Gironde estuary: a recent model for macrotidal estuarine systems. In: Smith, D.G., Zaitlin, B.A., Reinson, G.E., Rahmani, R.A. (Eds.), *Clastic Tidal Sedimentology — Recognition Criteria and Facies Models* 16. pp. 29–39. *Mem. Can. Soc. Petrol. Geol.*
- Alqahtani, F.A., Johnson, H.D., Jackson, C.A.-L., Som, M.R.B., 2015. Nature, origin and evolution of a late pleistocene incised valley-fill, Sunda Shelf, Southeast Asia. *Sedimentology* 62, 1198–1232.
- Amorosi, A., Sarti, G., Rossi, V., Fontana, V., 2008. Anatomy and sequence stratigraphy of the late quaternary Arno valley fill (Tuscany, Italy). In: Amorosi, A., Haq, B.U., Sabato, L. (Eds.), *Advances in Application of Sequence Stratigraphy in Italy* 1. *GeoActa Special Publication*, pp. 117–128.
- Amorosi, A., Pacifico, A., Rossi, V., Ruberti, D., 2012. Late Quaternary incision and deposition in an active volcanic setting: the Volturno valley fill, Southern Italy. *Sediment. Geol.* 282, 307–320.
- Amorosi, A., Rossi, V., Sarti, G., Mattei, R., 2013. Coalescent valley fills from the late Quaternary record of Tuscany (Italy). *Quat. Int.* 288, 129–138.
- Amorosi, A., Bracone, V., Campo, B., D'Amico, C., Rossi, V., Roskopf, C.M., 2016. A late Quaternary multiple paleovalley system from the Adriatic coastal plain (Biferno River, Southern Italy). *Geomorphology* 254, 146–159.
- Anderson, J.B., Siringan, F.P., Taviani, M., Lawrence, J., 1991. Origin and evolution of Sabine Lake, Texas-Louisiana. *Gulf Coast Assoc. Geol. Soc. Trans.* 41, 12–16.
- Becker, J.J., Sandwell, D.T., Smith, W.H.F., Braud, J., Binder, B., Depner, J., Fabre, D., Factor, J., Ingalls, S., Kim, S.H., Ladner, R., Marks, K., Nelson, S., Pharaoh, A., Trimmer, R., Von Rosenberg, J., Wallace, G., Weatherall, P., 2009. Global bathymetry and elevation data at 30 arc seconds resolution: SRTM30 PLUS. *Mar. Geodesy* 32, 355–371.
- Belknap, D.F., Kraft, J.C., 1981. Preservation potential of transgressive coastal lithosomes on the US Atlantic shelf. *Mar. Geol.* 42, 429–442.
- Bellotti, P., Caputo, C., Davoli, L., Evangelista, S., Garzanti, E., Pugliese, F., Valeri, P., 2004. Morpho-sedimentary characteristics and Holocene evolution of the emergent part of the Ombrone River delta (southern Tuscany). *Geomorphology* 61, 71–90.
- Benallack, K., Green, A.N., Humphries, M.S., Cooper, J.A.G., Dladla, N.N., Finch, J.M., 2016. The stratigraphic evolution of a large back-barrier lagoon system with a non-migrating barrier. *Mar. Geol.* 379, 64–77.
- Berné, S., Vagner, P., Guichard, F., Lericolais, G., Liu, Z., Trentesaux, A., Yin, P., Yi, H.I., 2002. Pleistocene forced regressions and tidal sand ridges in the East China Sea. *Mar. Geol.* 188, 293–315.
- Blum, M.D., Price, D.M., 1998. Quaternary alluvial plain construction in response to interacting glacio-eustatic and climatic controls, Texas Gulf coastal Plain. In: Shanley, K.W., McCabe, P.J. (Eds.), *Relative Role of Eustasy, Climate and Tectonism in Continental Rocks* 59. SEPM Spec. Publ., pp. 31–48.
- Blum, M.D., Womack, J.H., 2009. Climate change, sea-level change, and fluvial sediment supply to deepwater systems. In: Kneller, B., Martinsen, O.J., McCaffrey, B. (Eds.), *External Controls on Deep Water Depositional Systems: Climate, Sea-Level, and Sediment Flux* 92. SEPM Spec. Publ., pp. 15–39.
- Blum, M., Martin, J., Milliken, K., Garvin, M., 2013. Paleovalley systems: insights from Quaternary analogs and experiments. *Earth-Sci. Rev.* 116, 128–169.
- Bowen, D.W., Weimer, P., 2003. Regional sequence stratigraphic setting and reservoir geology of Morrow incised-valley sandstones (lower Pennsylvanian), eastern Colorado and western Kansas. *AAPG Bull.* 87, 781–815.
- Breda, A., Amorosi, A., Rossi, V., Fusco, F., 2016. Late-glacial to Holocene depositional architecture of the Ombrone paleovalley system (Southern Tuscany, Italy): sea-level, climate and local control in valley-fill variability. *Sedimentology* 63, 1124–1148.
- Bridge, J.S., Mackey, S.D., 1993. A theoretical study of fluvial sandstone body dimensions. In: Flint, S.S., Bryant, L.D. (Eds.), *Geological Modeling of Hydrocarbon Reservoirs and Outcrop Analogues* 15. *Int. Assoc. Sedimentol. Spec. Publ.*, pp. 213–236.
- Burgess, P.M., Steel, R.J., Granjeon, D., 2008. Stratigraphic forward modeling of basin-margin clinoform systems: implications for controls on topset and shelf width and timing of formation of shelf-edge deltas. In: Hampson, G.J., Steel, R.J., Burgess, P.M., Dalrymple, R.W. (Eds.), *Recent Advances in Models of Siliciclastic Shallow-Marine Stratigraphy* 90. SEPM Spec. Publ., pp. 35–45.
- Carlin, J.A., Dellapenna, T.M., Strom, K., Noll, C.J.I., 2015. The influence of a salt wedge intrusion on fluvial suspended sediment and the implications for sediment transport to the adjacent coastal ocean: a study of the lower Brazos River TX, USA. *Mar. Geol.* 359, 134–147.
- Cattaneo, A., Steel, R.J., 2003. Transgressive deposits: a review of their variability. *Earth-Sci. Rev.* 62, 187–228.
- Cawthra, H.C., Uken, R., 2012. Modern beachrock formation in Durban, KwaZulu-Natal. *S. Afr. J. Sci.* 108, 1–5.
- Chaumillon, E., Weber, N., 2006. Spatial variability of modern incised valleys on the French Atlantic Coast: comparison between the charente and the Lay-Sèvre incised valleys. In: Dalrymple, R.W., Leckie, D.A., Tillman, R.W. (Eds.), *Incised Valleys in Time and Space* 85. SEPM Special Publication, pp. 57–85.
- Chaumillon, E., Proust, J.N., Menier, D., Weber, N., 2008. Incised-valley morphologies and sedimentary-fills within the inner shelf of the Bay of Biscay (France): a synthesis. *J. Mar. Syst.* 72, 383–396.
- Chaumillon, E., Tessier, B., Reynaud, J.Y., 2010. Stratigraphic records and variability of incised valleys and estuaries along French coasts. *Bulletin de la Société géologique de France* 181, 75–85.
- Cilumbriello, A., Sabato, L., Tropeano, M., Gallicchio, S., Grippa, A., Maiorano, P., Mateu-Vicens, G., Rossi, C.A., Spilotro, G., Calcagnile, L., Quarta, G., 2010. Sedimentology, stratigraphic architecture and preliminary hydrostratigraphy of the Metaponto coastal-plain subsurface (Southern Italy). *Memorie Descrittive della Carta Geologica*

- d'Italia XC, 67–84.
- Clement, A.J., Fuller, I.C., 2018. Influence of system controls on the Late Quaternary geomorphic evolution of a rapidly-infilled incised-valley system: the lower Manawatu valley, North Island New Zealand. *Geomorphology* 303, 13–29.
- Clement, A.J., Fuller, I.C., Sloss, C.R., 2017. Facies architecture, morphostratigraphy, and sedimentary evolution of a rapidly-infilled Holocene incised-valley estuary: the lower Manawatu valley, North Island New Zealand. *Mar. Geol.* 390, 214–233.
- Colombera, L., Mountney, N.P., Hodgson, D.M., McCaffrey, W.D., 2016. The Shallow-Marine Architecture Knowledge Store: a database for the characterization of shallow-marine and paralic depositional systems. *Mar. Petrol. Geol.* 75, 83–99.
- Cooper, W.S., 1958. Coastal sand dunes of Oregon and Washington. *Memoir-Geol. Soc. Am.* 72, 144.
- Cooper, J.A.G., 1991. Beachrock formation in low latitudes: implications for coastal evolutionary models. *Mar. Geol.* 98, 145–154.
- Cooper, J.A.G., Green, A.N., Meireles, R.P., Klein, A.H., Souza, J., Toldo, E.E., 2016. Sandy barrier overstepping and preservation linked to rapid sea level rise and geological setting. *Mar. Geol.* 382, 80–91.
- Cowell, P.J., Thom, B.G., 1994. Morphodynamics of coastal evolution. In: Carter, R.W.G., Woodroffe, C.D. (Eds.), *Coastal Evolution, Late Quaternary Shoreline Morphodynamics*. Cambridge University Press, Cambridge, pp. 33–86.
- Dalrymple, R.W., 2006. Incised valleys in space and time: an introduction to the volume and an examination of the controls on valley formation and filling. In: In: Dalrymple, R.W., Leckie, D.A., Tillman, R.W. (Eds.), *Incised Valleys in Space and Time 85*. SEPM Spec. Publ., pp. 5–12.
- Dalrymple, R.W., Zaitlin, B.A., Boyd, R., 1992. Estuarine facies models: conceptual basis and stratigraphic implications. *J. Sed. Petrol.* 62, 1130–1146.
- Dalrymple, R.W., Boyd, R., Zaitlin, B.A., 1994. Preface. In: In: Dalrymple, R.W., Boyd, R., Zaitlin, B.A. (Eds.), *Incised Valley Systems: Origins and Sedimentary Sequences 51*. SEPM Spec. Publ., pp. iii.
- Dalrymple, R.W., Baker, E.K., Harris, P.T., Hughes, M., 2003. Sedimentology and stratigraphy of a tide-dominated, foreland-basin delta (fly River, Papua New Guinea). In: In: Sidi, F.H., Nummedal, D., Imbert, P., Darman, H., Posamentier, H.W. (Eds.), *Tropical Deltas of Southeast Asia – Sedimentology, Stratigraphy, and Petroleum Geology 76*. SEPM Spec. Publ., pp. 147–173.
- Dalrymple, R.W., Mackay, D.A., Ichaso, A.A., Choi, K.S., 2012. Processes, morphodynamics, and facies of tide-dominated estuaries. In: Davis Jr.R.A., Dalrymple, R.W. (Eds.), *Principles of Tidal Sedimentology*. Springer, Dordrecht, Heidelberg, pp. 79–107.
- Dalrymple, R.W., Zaitlin, B.A., 1994. High-resolution sequence stratigraphy of a complex, incised valley succession, the Cobequid Bay–Salmon River estuary, Bay of Fundy, Canada. *Sedimentol.* 41, 1069–1091.
- Davis Jr, R.A., Clifton, H.E., 1987. Sea-level change and the preservation potential of wave-dominated and tide-dominated coastal sequences. In: In: Nummedal, D., Pilkey, O.H., Howard, J.D. (Eds.), *Sea-Level Fluctuation and Coastal Evolution 41*. Society of Economic Palaeontologists and Mineralogists Special Publication, pp. 167–178.
- Davis Jr, R.A., FitzGerald, D.M., 2009. *Beaches and Coasts*. John Wiley & Sons.
- Davis Jr, R.A., Hayes, M.O., 1984. What is a wave-dominated coast? *Mar. Geol.* 60, 313–329. [https://doi.org/10.1016/0025-3227\(84\)90155-5](https://doi.org/10.1016/0025-3227(84)90155-5).
- Davis, J.C., Sampson, R.J., 2002. *Statistics and Data Analysis in Geology*, 3rd ed. Wiley, New York.
- Dietrich, W.E., Whiting, P., 1989. Boundary shear stress and sediment transport in river meanders of sand and gravel. In: In: Ikeda, H., Parker, G. (Eds.), *River Meandering: AGU Water Resources Monograph 12*. pp. 1–50.
- Féniès, H., Lericolais, G., 2005. Internal architecture of an incised valley-fill on a wave- and tide-dominated coast (the Leyre incised valley, Bay of Biscay, France). *Comptes Rendus Geosci.* 337, 1257–1266.
- Féniès, H., Tastet, J., 1998. Facies and architecture of an estuarine tidal bar (the Trompeloup bar, Gironde Estuary, SW France). *Mar. Geol.* 150, 149–169.
- Féniès, H., Lericolais, G., Posamentier, H.W., 2010. Comparison of wave- and tide-dominated incised valleys: specific processes controlling systems tract architecture and reservoir geometry. *Bulletin de la Société Géologique de France* 181, 171–181.
- Ferrer, P., Benabdellouahed, M., Certain, R., Tessier, B., Barusseau, J.P., Bouchette, F., 2010. The Late Holocene sediment infilling and beach barrier dynamics of the Thau lagoon (Gulf of Lions, Mediterranean Sea, SE France). *Bulletin de la Société Géologique de France* 181, 197–209.
- Fielding, C.R., Crane, R.C., 1987. An application of statistical modelling to the prediction of hydrocarbon recovery factors in fluvial reservoir sequences. In: In: Ethridge, F.G., Flores, R.M., Harvey, M.D. (Eds.), *Recent Developments in Fluvial Sedimentology 39*. SEPM Spec. Publ., pp. 321–327.
- Fielding, C.R., Trueman, J.D., Alexander, J., 2006. Holocene depositional history of the Burdekin river delta of northeastern Australia: a model for a lowaccommodation, highstand delta. *J. Sed. Res.* 76, 411–428.
- Forbes, D.L., Orford, J.D., Carter, R.W.G., Shaw, J., Jennings, S.C., 1995. Morphodynamic evolution, self-organisation, and instability of coarse-clastic barriers on paraglacial coasts. *Mar. Geol.* 126, 63–85.
- Frankel, E., 1968. Rate of formation of beachrock. *Earth Planet. Sci. Lett.* 4, 439–440.
- Gardner, J.V., Dartnell, P., Mayer, L.A., Hughes-Clarke, J.E., Calder, B.R., Duffy, G., 2005. Shelf-edge deltas and drowned barrier-island complexes on the northwest Florida outer continental shelf. *Geomorphology* 64, 133–166.
- Gardner, J.V., Calder, B.R., Hughes Clark, J.E., Mayer, L.A., Elston, G., Rzhonov, Y., 2007. Drowned shelf-edge deltas, barrier islands and related features along the outer continental shelf north of the head of De Soto Canyon, NE Gulf of Mexico. *Geomorphology* 89, 370–390.
- Geehan, G., Underwood, J., 1993. The use of shale length distributions in geological modeling. In: In: Flint, S., Bryant, I.D. (Eds.), *The Geological Modeling of Hydrocarbon Reservoirs and Outcrop Analogues 15*. Int. Assoc. Sedimentol. Spec. Publ., pp. 205–212.
- Gibling, M.R., 2006. Width and thickness of fluvial channel bodies and valley fills in the geological record: a literature compilation and classification. *J. Sediment. Res. A Sediment. Petrol. Process.* 76, 731–770.
- Green, A.N., 2009. Palaeo-drainage, incised valley fills and transgressive systems tract sedimentation of the northern KwaZulu-Natal continental shelf, South Africa, SW Indian Ocean. *Mar. Geol.* 263, 46–63.
- Green, A., Garlick, G.L., 2011. A sequence stratigraphic framework for a narrow, current-swept continental shelf: the Durban Bight, central KwaZulu-Natal, South Africa. *J. Afr. Earth Sci.* 60, 303–314.
- Green, A.N., Cooper, J.A.G., Salzmann, L., 2014. Geomorphic and stratigraphic signals of postglacial meltwater pulses on continental shelves. *Geology* 42, 151–154.
- Green, A.N., Cooper, J.A.G., Wiles, E.A., De Lecea, A.M., 2015. Seismic architecture, stratigraphy and evolution of a subtropical marine embayment: maputo Bay, Mozambique. *Mar. Geol.* 369, 300–309.
- Green, A.N., Cooper, J.A.G., Salzmann, L., 2018. The role of shelf morphology and antecedent setting in the preservation of palaeo-shoreline (beachrock and aeolianite) sequences: the SE African shelf. *Geo-Marine Lett.* 38, 5–18.
- Green, A.N., Cooper, J.A.G., Leuci, R., Thackeray, Z., 2013a. Formation and preservation of an overstepped segmented lagoon complex on a high-energy continental shelf. *Sedimentology* 60, 1755–1768.
- Green, A.N., Dladla, N., Garlick, G.L., 2013b. Spatial and temporal variations in incised valley systems from the Durban continental shelf, KwaZulu-Natal, South Africa. *Mar. Geol.* 335, 148–161.
- Greene Jr, D.L., Rodriguez, A.B., Anderson, J.B., 2007. Seaward-branching coastal-plain and piedmont incised-valley systems through multiple sea-level cycles: Late Quaternary examples from Mobile Bay and Mississippi Sound, USA. *J. Sediment. Res.* 77, 139–158.
- Grippa, A., Bianca, M., Tropeano, M., Cilumbriello, A., Gallipoli, M.R., Mucciarelli, M., Sabato, L., 2011. Use of the HVSR method to detect buried paleomorphologies (filled incised-valleys) below a coastal plain: the case of the Metaponto plain (Basilicata, southern Italy). *Bollettino di Geofisica Teorica ed Applicata* 52, 225–240.
- Hampson, G.J., Davies, S.J., Elliott, T., Flint, S.S., Stollhofen, H., 1999. Incised valley fill sandstone bodies in Upper Carboniferous fluvio-deltaic strata: recognition and reservoir characterization of Southern North Sea analogues. In: Geological Society, London, Petroleum Geology Conference Series. Geological Society of London. pp. 771–788 Vol. 5, No. 1.
- Harris, P.T., Macmillan-Lawler, M., Rupp, J., Baker, E.K., 2014. Geomorphology of the oceans. *Mar. Geol.* 352, 4–24.
- Healy, T., Harada, K., 1991a. Definition and physical characteristics of the world's enclosed coastal seas. *Mar. Pollut. Bull.* 23, 639–644.
- Healy, T., Harada, K., 1991b. Enclosed and semi-enclosed coastal seas. *J. Coast. Res.* 7, i–vi.
- Healy, T., Werner, F., 1987. Sediment budget for a semi-enclosed sea in a near homogeneous lithology; example of Kieler Bucht, Western Baltic. *Senckenberg. Marit.* 19, 32–70.
- Heap, A.D., Nichol, S.L., 1997. The influence of limited accommodation space on the stratigraphy of an incised-valley succession: weiti River estuary, New Zealand. *Mar. Geol.* 144, 229–252.
- Helland-Hansen, W., Martinsen, O.J., 1996. Shoreline trajectories and sequences: description of variable depositional-dip scenarios. *J. Sediment. Res. A Sediment. Petrol. Process.* 66, 670–688.
- Helland-Hansen, W., Steel, R.J., Somme, T.O., 2012. Shelf genesis revisited. *J. Sed. Res.* 82, 133–148.
- Hopley, D., 1986. Beachrock as a sea-level indicator. In: van de Plassche, O. (Ed.), *Sealevel Research: A Manual for the Collection and Evaluation of Data*. Geo Books, Regency House, Norwich, pp. 157–173.
- Houbolt, J.J.H.C., 1968. Recent sediments in the southern bight of the North Sea. *Geol. Mijnb.* 47, 245–273.
- Hori, K., Saito, Y., Zhao, Q., Wang, P., 2002. Architecture and evolution of the tide-dominated Changjiang (Yangtze) River delta. *China Sed. Geol.* 146, 249–264.
- Hume, T.M., 2005. Tidal prism. In: Schwartz, M.L. (Ed.), *Encyclopedia of Coastal Science*. Encyclopedia of Earth Science Series. Springer, Dordrecht.
- Ishihara, T., Sugai, T., 2017. Eustatic and regional tectonic controls on late Pleistocene paleovalley morphology in the central Kanto Plain, Japan. *Quat. Int.* 456, 69–84.
- Ishihara, T., Sugai, T., Hachinohe, S., 2012. Fluvial response to sea-level changes since the latest Pleistocene in the near-coastal lowland, central Kanto Plain, Japan. *Geomorphology* 147, 49–60.
- Kennedy, D.M., Paulik, R., Millar, M., 2008. Infill of a structurally controlled estuary: an example from southern Whanganui Inlet, New Zealand. *N. Z. Geogr.* 64, 20–33.
- Kennish, M.J., 1991. *Ecology of Estuaries: Anthropogenic Effects Vol. 1* CRC press.
- Korus, J.T., Kvale, E.P., Eriksson, K.A., Joeckel, R.M., 2008. Compound paleovalley fills in the Lower Pennsylvanian New River Formation, West Virginia, USA. *Sed. Geol.* 208, 15–26.
- Leckie, D.A., 1994. Canterbury Plains, New Zealand — implications for sequence stratigraphic models. *AAPG Bull.* 78, 1240–1252.
- Lericolais, G., Berné, S., Féniès, H., 2001. Seaward pinching out and internal stratigraphy of the Gironde incised valley on the shelf (Bay of Biscay). *Mar. Geol.* 175, 183–197.
- Li, C.X., Wang, P.X., 1998. Late Quaternary Stratigraphy of the Yangtze Delta. *China Science Press, Beijing*, pp. 222pp.
- Li, C., Wang, P., Sun, H., Zhang, J., Fan, D., Deng, B., 2002. Late Quaternary incised-valley fill of the Yangtze delta (China): its stratigraphic framework and evolution. *Sediment. Geol.* 152, 133–158.
- Li, C., Wang, P., Fan, D., Yang, S., 2006. Characteristics and formation of late quaternary incised-valley-fill sequences in sediment-rich deltas and estuaries: case studies from

- China. In: In: Dalrymple, R.W., Leckie, D.A., Tillman, R.W. (Eds.), *Incised Valleys in Time and Space 85*. SEPM Special Publication, pp. 141–160.
- Lin, C.M., Zhuo, H.C., Gao, S., 2005. Sedimentary facies and evolution in the Qiantang River incised valley, eastern China. *Mar. Geol.* 219 (4), 235–259.
- Luketina, D., 1998. Simple tidal prism models revisited. *Estuar. Coast. Shelf Sci.* 46, 77–84.
- Marlianingrum, P.R., Kusumastanto, T., Adrianto, L., Fahrudin, A., 2019. Economic analysis of management option for sustainable mangrove ecosystem in Tangerang District, Banten Province, Indonesia. In: *IOP Conference Series: Earth and Environmental Science*. IOP Publishing. Vol. 241, No. 1, p. 012026.
- Martin, J., Cantelli, A., Paola, C., Blum, M., Wolinsky, M., 2011. Quantitative modeling of the evolution and geometry of incised valleys. *J. Sediment. Res.* 81, 64–79.
- Maselli, V., Trincardi, F., 2013. Large-scale single incised valley from a small catchment basin on the western Adriatic margin (central Mediterranean Sea). *Glob. Planet. Change* 100, 245–262.
- Maselli, V., Trincardi, F., Asioli, A., Ceregato, A., Rizzetto, F., Taviani, M., 2014. Delta growth and river valleys: the influence of climate and sea level changes on the South Adriatic shelf (Mediterranean Sea). *Quat. Sci. Rev.* 99, 146–163.
- Masselink, G., Hughes, M.G., 2003. *Introduction to Coastal Processes and Geomorphology*. Oxford University Press, New York, pp. 354 p.
- Matheus, C.R., Rodriguez, A.B., 2011. Controls on late Quaternary incised-valley dimension along passive margins evaluated using empirical data. *Sedimentology* 58, 1113–1137.
- Matheus, C.R., Rodriguez, A.B., 2014. Controls on lower-coastal-plain valley morphology and fill architecture. *J. Sediment. Res.* 84, 314–325.
- Matheus, C.R., Rodriguez, A.B., Greene, D.L., Simms, A.R., Anderson, J.B., 2007. Control of upstream variables on incised-valley dimension. *J. Sediment. Res.* 77, 213–224.
- Menier, D., 2004. Morphologie et remplissage des vallées fossiles sud-armoricaines: apport de la stratigraphie sismique. PhD Thesis. Université de Bretagne Sud.
- Menier, D., Reynaud, J.-Y., Proust, J.-N., Guillocheau, F., Guennoc, P., Bonnet, S., Tessier, B., Goubert, E., 2006. Basement control on shaping and infilling of valleys incised at the southern coast of Brittany, France. In: In: Dalrymple, R.W., Leckie, D.A., Tillman, R.W. (Eds.), *Incised Valleys in Time and Space 85*. SEPM Special Publication, pp. 37–55.
- Menier, D., Tessier, B., Proust, J.N., Baltzer, A., Sorrel, P., Traini, C., 2010. The Holocene transgression as recorded by incised-valley infilling in a rocky coast context with low sediment supply (southern Brittany, western France). *Bulletin de la Société Géologique de France* 181, 115–128.
- Milli, S., D'Ambrogio, C., Bellotti, P., Calderoni, G., Carboni, M.G., Celant, A., Di Bella, L., Di Rita, F., Frezza, V., Magri, D., Pichezzi, R.M., Ricci, V., 2013. The transition from wave-dominated estuary to wave-dominated delta: the Late Quaternary stratigraphic architecture of Tiber River deltaic succession (Italy). *Sediment. Geol.* 284, 159–180.
- Milli, S., Mancini, M., Moscatelli, M., Stigliano, F., Marini, M., Cavinato, G.P., 2016. From river to shelf, anatomy of a high-frequency depositional sequence: the Late Pleistocene to Holocene Tiber depositional sequence. *Sedimentology* 63, 1886–1928.
- Milliman, J.D., Syvitski, J.P.M., 1992. Geomorphic/tectonic control of sediment discharge to the oceans: the importance of small mountainous rivers. *J. Geol.* 100, 525–544.
- Moore, C.H., 2001. Carbonate reservoir porosity evolution and diagenesis in a sequence stratigraphic framework. In: In: van Loon, A.J. (Ed.), *Developments in Sedimentology* 55. Elsevier, Doorwerth, Netherlands, pp. 185–244.
- Nichol, S.L., Boyd, R., Penland, S., 1996. Sequence stratigraphy of a coastal-plain incised valley estuary, Lake Calcasieu, Louisiana. *J. Sediment. Res.* 66, 847–857.
- Nordfjord, S., Goff, J.A., Austin, J.A., Sommerfield, C.K., 2005. Seismic geomorphology of buried channel systems on the New Jersey outer shelf: assessing past environmental conditions. *Mar. Geol.* 214, 339–364.
- Nordfjord, S., Goff, J.A., Austin, J.A., Gulick, S.P.S., 2006. Seismic facies of incised-valley fills, New Jersey continental shelf: implications for erosion and preservation processes acting during latest Pleistocene–holocene transgression. *J. Sediment. Res.* 76, 1284–1303.
- Olariu, C., Steel, R.J., 2009. Influence of point-source sediment-supply on modern shelf-slope morphology: implications for interpretation of ancient shelf margins. *Basin Res.* 21, 484–501.
- Olariu, C., Steel, R.J., Dalrymple, R.W., Gings, M.K., 2012. Tidal dunes versus tidal bars: the sedimentological and architectural characteristics of compound dunes in a tidal seaway, the lower Baronia Sandstone (Lower Eocene), Ager Basin, Spain. *Sediment. Geol.* 279, 134e155.
- Payenberg, T.H., Boyd, R., Beaudoin, J., Ruming, K., Davies, S., Roberts, J., Lang, S.C., 2006. The filling of an incised valley by shelf dunes — an example from Hervey Bay, east coast of Australia. In: In: Dalrymple, R.W., Leckie, D.A., Tillman, R.W. (Eds.), *Incised Valleys in Time and Space 85*. SEPM Special Publication, pp. 87–98.
- Peakall, J., Ashworth, P.J., Best, J.L., 2007. Meanderbend evolution, alluvial architecture, and the role of cohesion in sinuous river channels: a flume study. *J. Sediment. Res. A* 177, 197–212.
- Phillips, J.D., 2011. Drainage area and incised valley fills in Texas rivers: a potential explanation. *Sed. Geol.* 242, 65–70.
- Portela, L.I., Ramos, S., Teixeira, A.T., 2013. Effects of salinity on the settling velocity of fine sediments of a harbour basin. *J. Coastal Res.* 65, 1188–1193.
- Posamentier, H.W., 2001. Lowstand alluvial bypass systems: incised vs. unincised. *AAPG Bull.* 85, 1771–1793.
- Posamentier, H.W., Allen, G.P., 1999. *Siliciclastic Sequence Stratigraphy: Concepts and Applications* Vol. 7. SEPM (Society for Sedimentary Geology), Tulsa, Oklahoma, pp. 210.
- Pretorius, L., Green, A., Cooper, A., 2016. Submerged shoreline preservation and ravinement during rapid postglacial sea-level rise and subsequent “slowstand”. *GSA Bull.* 128, 1059–1069.
- Proust, J.N., Menier, D., Guillocheau, F., Guennoc, P., Bonnet, S., Rouby, D., Le Corre, C., 2001. Fossil valleys in the bay of Vilaine (Brittany, France): nature and evolution of the Pleistocene coastal sediment wedge of Brittany. *Bulletin de la Société Géologique de France* 172 (6), 737–749.
- Proust, J.N., Renault, M., Guennoc, P., Thion, I., 2010. Sedimentary architecture of the Loire River drowned valleys of the French Atlantic shelf. *Bulletin de la Société géologique de France* 181, 129–149.
- R Core Team, 2019. *R: a Language and Environment for Statistical Computing*. R Foundation for Statistical Computing, Vienna, Austria (Accessed 21 August 2019). <https://www.R-project.org/>.
- Ray, N., Adams, J., 2001. A GIS-based vegetation map of the world at the last glacial maximum (25,000–15,000 BP). *Int. Archaeol. pp.* 11. Available at: <http://intarch.ac.uk/journal/issue11/bristowpindex.html>.
- Reading, H.G., Collinson, J.D., 1996. *Clastic coasts*. In: Reading, H.G. (Ed.), *Sedimentary Environments: Processes, Facies and Stratigraphy*. Blackwell Science, Oxford, pp. 154–231.
- Reijnenstein, H.M., Posamentier, H.W., Bhattacharya, J.P., 2011. Seismic geomorphology and high-resolution seismic stratigraphy of inner-shelf fluvial, estuarine, deltaic, and marine sequences, Gulf of Thailand. *Bull.* 95, 1959–1990.
- Rodriguez, A.B., Anderson, J.B., Siringan, F.P., Taviani, M., 1999. Sedimentary Facies and Genesis of Holocene Sand Bankson the East Texas Inner Continental Shelf. In: In: Snedden, J., Bergman, K. (Eds.), *Isolated Shallow Marine Sand Bodies: Sequence Stratigraphic Analysis and Sedimentologic Interpretation* 64. SEPM Special Publications, pp. 165–178.
- Rodriguez, A.B., Anderson, J.B., Simms, A.R., 2005. Terrace inundation as an autocyclic mechanism for parasequence formation: galveston Estuary, Texas, USA. *J. Sediment. Res.* 75, 608–620.
- Rodriguez, A.B., Duran, D.M., Matheus, C.R., Anderson, J.B., 2008. Sediment accommodation control on estuarine evolution: an example from weeks Bay, Alabama, USA. In: In: Anderson, J.B., Rodriguez, A.B. (Eds.), *Response of Upper Gulf Coast Estuaries to Holocene Climate Change and Sea-Level Rise*. Special Paper of the Geological Society of America 443, pp. 31–42.
- Rossi, V., Amorosi, A., Sarti, G., Mariotti, S., 2017. Late Quaternary multiple incised-valley systems: an unusually well-preserved stratigraphic record of two interglacial valley-fill successions from the Arno plain (northern Tuscany, Italy). *Sedimentology* 64, 1901–1928.
- Roy, P.S., 1984. New South Wales Estuaries: their origin and evolution. In: Thom, B.G. (Ed.), *Coastal Geomorphology in Australia*. Academic Press, Sydney, NSW, pp. 99–121.
- Sakai, T., Fujiwara, O., Kamataki, T., 2006. Incised-valley-fill succession affected by rapid tectonic uplifts: an example from the uppermost Pleistocene to Holocene of the Isumi River lowland, central Boso Peninsula, Japan. *Sediment. Geol.* 185, 21–39.
- Salem, A.M., Ketzer, J.M., Morad, S., Rizk, R.R., Al-Aasm, I.S., 2005. Diagenesis and reservoir-quality evolution of incised-valley sandstones: evidence from the Abu Madi gas reservoirs (Upper Miocene), the Nile Delta basin, Egypt. *J. Sediment. Res.* 75, 572–584.
- Salzmann, L., Green, A., Cooper, J.A.G., 2013. Submerged barrier shoreline sequences on a high energy, steep and narrow shelf. *Mar. Geol.* 346, 366–374.
- Schumm, S.A., Brackenkridge, S.A., 1987. River response. North America and adjacent oceans during the last deglaciation. In: Ruddiman, W.F., Wright JrH.E. (Eds.), *Geol. Soc. Am. The Geology of North America*, pp. 221–240 K-3.
- Schwartz, M.L., 2005. *Encyclopedia of Coastal Science*. Springer Science & Business Media, Dordrecht.
- Shanley, K.W., 2004. *Fluvial Reservoir Description for a Giant, Low-permeability Gas Field*. Jonah Field, Green River Basin, WY.
- Shanley, K.W., McCabe, P.J., 1994. Perspectives on the sequence stratigraphy of continental strata: report of a working group at the 1991 NUNA conference of high-resolution sequence stratigraphy. *AAPG Bull.* 78, 544–568.
- Sheets, B.A., Hickson, T.A., Paola, C., 2002. Assembling the stratigraphic record: depositional patterns and timescales in an experimental alluvial basin. *Basin Res.* 14, 287–301.
- Simms, A.R., 2005. *Late Quaternary/Holocene Evolution of the Nueces Incised Valley, Central Texas*. PhD Thesis. Rice University, Houston.
- Simms, A.R., Anderson, J.B., Taha, Z.P., Rodriguez, A.B., 2006. Overfilled versus underfilled incised valleys: examples from the Quaternary Gulf of Mexico. In: In: Dalrymple, R.W., Leckie, D.A., Tillman, R.W. (Eds.), *Incised Valleys in Time and Space 85*. SEPM Special Publication, pp. 117–139.
- Simms, A.R., Aryal, N., Miller, L., Yokoyama, Y., 2010. The incised valley of Baffin Bay, Texas: a tale of two climates. *Sedimentology* 57, 642–669.
- Sloss, C.R., Jones, B.G., Murray-Wallace, C.V., McClennen, C.E., 2005. Holocene sea level fluctuations and the sedimentary evolution of a barrier estuary: Lake Illawarra, New South Wales, Australia. *J. Coast. Res.* 21, 943–959.
- Sloss, C.R., Jones, B.G., McClennen, C.E., de Carli, J., Price, D.M., 2006. The geomorphological evolution of a wave-dominated barrier estuary: burrill Lake, New South Wales, Australia. *Sediment. Geol.* 187, 229–249.
- Sloss, C.R., Jones, B.G., Switzer, A.D., Nichol, S., Clement, A.J., Nicholas, A.W., 2010. The Holocene infill of Lake Conjola, a narrow incised valley system on the southeast coast of Australia. *Quat. Int.* 221, 23–35.
- Smyth, W.C., 1991. *Seismic facies analysis and depositional history of an incised valley system*. Galveston Bay area, Texas. Rice University, Houston PhD Thesis.
- Sømme, T.O., Helland-Hansen, W., Martinsen, O.J., Thurmond, J.B., 2009a. Relationships between morphological and sedimentological parameters in source-to-sink systems: a basis for predicting semi-quantitative characteristics in subsurface systems. *Basin Res.* 21, 361–387.
- Sømme, T.O., Martinsen, O.J., Thurmond, J.B., 2009b. Reconstructing morphological and depositional characteristics in subsurface sedimentary systems: an example from the

- Maastrichtian-Danian Ormen Lange system, Møre Basin, Norwegian Sea. *AAPG Bull.* 93, 1347–1377.
- Stephen, K.D., Dalrymple, M., 2002. Reservoir simulations developed from an outcrop of incised valley fill strata. *Bull.* 86, 797–822.
- Stive, M.J.F., De Vriend, H.J., 1995. Modelling shoreface profile evolution. *Mar. Geol.* 126, 235–248.
- Storms, J.E.A., Weltje, G.J., Terra, G.J., Cattaneo, A., Trincardi, F., 2008. Coastal dynamics under conditions of rapid sea-level rise: late Pleistocene to Early Holocene evolution of barrier–lagoon systems on the northern Adriatic shelf (Italy). *Quat. Sci. Rev.* 27 (11–12), 1107–1123.
- Strong, N., Paola, C., 2008. Valleys that never were: time surfaces versus stratigraphic surfaces. *J. Sed. Res.* 78, 579–593.
- Syvitski, J.P.M., Milliman, J.D., 2007. Geology, geography, and humans battle for dominance over the delivery of fluvial sediment to the coastal ocean. *J. Geol.* 115, 1–19.
- Takashimizu, Y., Shibuya, T., Abe, Y., Otsuka, T., Suzuki, S., Ishii, C., Miyama, Y., Konishi, H., Hu, S.G., 2016. Depositional facies and sequence of the latest Pleistocene to Holocene incised valley fill in Kushiro Plain, Hokkaido, northern Japan. *Quat. Int.* 397, 159–172.
- Tanabe, S., Saito, Y., Vu, Q.L., Hanebuth, T.J., Ngo, Q.L., Kitamura, A., 2006. Holocene evolution of the Song Hong (Red River) delta system, northern Vietnam. *Sediment. Geol.* 187, 29–61.
- Tanabe, S., Nakanishi, T., Matsushima, H., Hong, W., 2013. Sediment accumulation patterns in a tectonically subsiding incised valley: insight from the Echigo Plain, central Japan. *Mar. Geol.* 336, 33–43.
- Tanabe, S., Nakanishi, T., Ishihara, Y., Nakashima, R., 2015. Millennial-scale stratigraphy of a tide-dominated incised valley during the last 14 kyr: spatial and quantitative reconstruction in the Tokyo Lowland, central Japan. *Sedimentology* 62, 1837–1872.
- Tessier, T., Billeaud, I., Sorrel, P., Delsinne, N., Lesueur, P., 2012. Infilling stratigraphy of macrotidal tide-dominated estuaries. Controlling mechanisms: sea-level fluctuations, bedrock morphology, sediment supply and climate changes (the examples of the Seine estuary and the Mont-Saint-Michel Bay, English Channel, NW France). *Sediment. Geol.* 279, 62–73.
- Tessier, B., Delsinne, N., Sorrel, P., 2010a. Holocene sedimentary infilling of a tide-dominated estuarine mouth. The example of the macrotidal Seine estuary (NW France). *Bull. Geol. Soc. France* 181, 87–98.
- Tessier, B., Billeaud, I., Lesueur, P., 2010b. Stratigraphic organization of a composite macrotidal wedge: the Holocene sedimentary infill of the Mont-Saint-Michel Bay. *Bull. Geol. Soc. France* 181, 99–113.
- Tesson, M., Labaune, C., Gensous, B., Delhaye-Prat, V., 2010. Quaternary compound incised valleys of the Roussillon coast (SE France): correlation of seismic data with core data. *Bulletin de la Société géologique de France* 181, 183–196.
- Thieler, E.R., Butman, B., Schwab, W.C., Allison, M.A., Driscoll, N.W., Donnelly, F.P., Uchupi, E., 2007. A catastrophic meltwater flood event and the formation of the Hudson Shelf Valley. *Palaeogeogr. Palaeoclimatol. Palaeoecol.* 246, 120–136.
- Thomas, M.A., Anderson, J.B., 1994. Sea-level controls on the facies architecture of the Trinity/Sabine incised-valley system Texas continental shelf. In: In: Dalrymple, R.W., Boyd, R., Zaitlin, B.A. (Eds.), *Incised-Valley Systems: Origin and Sedimentary Sequences* 51. SEPM Special Publications, pp. 64–82.
- Trincardi, F., Correggiari, A., Roveri, M., 1994. Late Quaternary transgressive erosion and deposition in a modern epicontinental shelf: the Adriatic semi-enclosed Basin. *Geomarine Lett.* 14, 41–51.
- Tropeano, M., Cilumbriello, A., Sabato, L., Gallicchio, S., Grippa, A., Longhitano, S.G., Bianca, M., Gallipoli, M.R., Mucciarelli, M., Spilotro, G., 2013. Surface and subsurface of the metaponto coastal plain (Gulf of Taranto—southern Italy): present-day-vs LGM-landscape. *Geomorphology* 203, 115–131.
- Van Wagoner, J.C., Mitchum, R.M., Campion, K.M., Rahmanian, V.D., 1990. Siliciclastic sequence stratigraphy in well logs, core, and outcrops: concepts for high resolution correlation of time and facies. *Am. Assoc. Petrol. Geol., Meth. Explor. Ser.* 7, 55.
- Vousdoukas, M.I., Velegrakis, A.F., Plomaritis, T.A., 2007. Beachrock occurrence, characteristics, formation mechanisms and impacts. *Earth. Rev.* 85, 23–46.
- Wang, R., Colombera, L., Mountney, N.P., 2019. Geological controls on the geometry of incised-valley fills: insights from a global dataset of late-Quaternary examples. *Sedimentology*. <https://doi.org/10.1111/sed.12596>. Published online early.
- Weber, N., Chaumillon, E., Tesson, M., Garlan, T., 2004. Architecture and morphology of the outer segment of a mixed tide and wave-dominated-incised valley, revealed by HR seismic reflection profiling: the paleo-Charente River, France. *Mar. Geol.* 207, 17–38.
- Wellner, R.W., Bartek, L.R., 2003. The effect of sea level, climate, and shelf physiography on the development of incised-valley complexes: a modern example from the East China Sea. *J. Sediment. Res.* 73, 926–940.
- Wetzal, A., Szczygielski, A., Unverricht, D., Stattegger, K., 2017. Sedimentological and ichnological implications of rapid Holocene flooding of a gently sloping mud-dominated incised valley—an example from the Red River (Gulf of Tonkin). *Sedimentology* 64, 1173–1202.
- Wilkinson, B.H., Byrne, J.R., 1977. Lavaca Bay – transgressive deltaic sedimentation in central Texas estuary. *AAPG Bull.* 61, 527–545.
- Wilson, K., Berryman, K., Cochran, U., Little, T., 2007. A Holocene incised valley infill sequence developed on a tectonically active coast: pakarae River, New Zealand. *Sediment. Geol.* 197, 333–354.
- Wood, L.J., Ethridge, F.G., Schumm, S.A., 1993. The effects of base-level fluctuations on coastal plain-shelfslope depositional systems: an experimental approach. In: In: Posamentier, H.W., Summerhayes, C.P., Haq, B.U., Allen, G.P. (Eds.), *Sequence Stratigraphy and Facies Associations* 18. Int. Assoc. Sedimentol. Spec. Publ., pp. 43–54.
- Yoshida, S., Steel, R., Dalrymple, R., Maceachern, J., 2005. Facies change between wave/storm- and tide/current-generated deposits within a relative sea level cycle: outcrop examples from the cretaceous Western interior seaway in North America—a review. *International Geological Programme 475 Delta Conference*.
- Zhang, G., Li, C., 1996. The fills and stratigraphic sequences in the Qiantangjiang incised paleovalley, China. *J. Sediment. Res.* 66, 406–414.
- Zaitlin, B.A., Dalrymple, R.W., Boyd, R., 1994. The stratigraphic organization of incised-valley systems associated with relative sea-level change. In: In: Dalrymple, R.W., Boyd, R., Zaitlin, B.A. (Eds.), *Incised-Valley Systems: Origin and Sedimentary Sequences* 51. SEPM Spec. Publ., pp. 45–60.
- Zhang, X., Lin, C.M., Dalrymple, R.W., Gao, S., Li, Y.L., 2014. Facies architecture and depositional model of a macrotidal incised-valley succession (Qiantang River estuary, eastern China), and differences from other macrotidal systems. *Bulletin* 126 (3-4), 499–522.
- Zhang, X., Dalrymple, R.W., Lin, C.M., 2017. Facies and stratigraphic architecture of the late Pleistocene to early Holocene tide-dominated paleo-Changjiang (Yangtze River) delta. *Geol. Soc. Am. Bull.* 130, 455–483.

Website

NOAA 2019: <https://tidesandcurrents.noaa.gov/map/index.html> (accessed 1 March 2019).

METOCEAN 2019: <https://app.metoceanview.com/hindcast/> (accessed 1 March 2019).